Exposure Design for Two-Sided Platforms*

Kei Ikegami†

January 2026

Abstract

Online platforms choose exposure rules—who is shown to whom and how often—to speed up matches and raise flow surplus. Yet aggressively matching today's best pairs can cannibalize future opportunities by thinning the effective option set for those who remain. I develop a two-sided sequential-search model with platform-controlled meeting propensities and define *user value* as the aggregate continuation value of search on the platform, a natural objective for platforms that seek to grow and retain users. I show that maximizing flow match surplus generally does not maximize user value, and I propose a tractable algorithm to compute user-value–optimal exposure via entropic regularization, annealing, and Bregman–Dykstra projections. Applying the framework to a doctor–spot-job platform, I estimate preferences under two exposure regimes and quantify the gains from redesigning exposure.

JEL Classification Codes: D47; D83; C78; J64; C61; C63; L86.

Keywords: two-sided platforms; sequential search; market design; matching; entropic optimal transport; recommendation systems; doctor–job matching.

1 Introduction

Online platforms are now ubiquitous in labor, dating, and product marketplaces. A core lever they control is the *exposure rule*—who is shown to whom, and how often—which is often tuned to accelerate promising encounters and increase match surplus. Yet an exposure rule that maximizes flow surplus need not be optimal from a longer-run perspective. Matching the very best pairs today can thin the effective option set faced by those who remain on the platform. Users may respond by lowering their acceptance thresholds, which can raise short-run match rates, but it also worsens future match prospects by leaving behind agents who would remain unmatched even under these lower standards. The result is dynamic cannibalization: current matches look strong, while the quality and likelihood of future matches deteriorate. This motivates an exposure-design question: what objective should a platform maximize, and how should exposure be designed to serve that objective?

I formalize and address these questions in a two-sided sequential-search framework à la Adachi (2003). I introduce the platform's exposure rule—governing pairwise meeting propensities—as a policy instrument. For any given exposure rule, the model pins down all participants' equilibrium continuation values.

*I am grateful to Medical Principle Co. for providing the data and for their thoughtful support in helping me understand the institutional background. I thank Yu Awaya, Michihiro Kandori, Fuhito Kojima, and Kyohei Okumura for valuable comments. I also thank participants at the ERATO meeting for helpful feedback.

†University of Tokyo, ikegamikei@e.u-tokyo.ac.jp

Their aggregate defines a long-run *user value*, which captures the expected gains from continued search and is a natural objective for a platform seeking to grow and retain its user base. The analysis shows that maximizing flow match surplus generally does not maximize user value, creating a wedge between short-run and long-run objectives. Building on this insight, I develop a tractable algorithm to compute the exposure rule that maximizes user value. Empirically, I study a doctor–spot-job matching platform. I estimate a structural model to recover participant preferences, and then solve the exposure-design problem to evaluate the gains from redesigning exposure rule.

Section 2 develops a sequential-search model in which, unlike the random matching of Adachi (2003), the platform can directly shape pairwise exposure propensities through an exposure rule. For any given rule, the model yields a system of Bellman equations that pins down the continuation values of all participants. I provide sufficient conditions under which this system has a stationary and unique solution. I also show, in a parametric example tailored to my empirical setting, that these conditions are plausibly satisfied in large markets.

Section 3 formalizes the cannibalization effect, poses the user–value maximization problem, and develops a tractable algorithm. I define long-run user value as the sum of participants' continuation values on the platform. Using this definition, I show that maximizing flow match surplus generally does not maximize user value. I solve the platform's problem of maximizing the user value via a regularization problem and taking its zero–temperature limit. The regularized problem admits a unique solution, and its zero–temperature limit solves the original problem. Furthermore, when the original problem has multiple solutions, the limit selects one according to a platform–chosen criterion such as equality across users or proximity to observed patterns. I then present a practical algorithm that implements the zero-temperature limit via annealing, while nesting the equilibrium computations required by the model. At each temperature level, the algorithm (i) solves for the continuation values as the fixed point induced by the current exposure rule and (ii) updates the exposure intensity by running Bregman–Dykstra KL projections to enforce the feasibility constraints that define the exposure rule (Benamou et al., 2014) .

Section 4 applies the algorithm to a doctor–spot-task platform. In the first half, I build a structural model of the platform. The data cover one month with 2,446 posts and 1,132 doctors. For each doctor–post pair, I observe the occurrence of an exposure and both sides' acceptance decisions. The market operates two exposure rules: (i) a self-search rule, under which doctors browse the website to find counterparts; and (ii) an agency-recommendation rule, under which agencies acting for medical institutions recommend doctors. I parameterize both exposure rules and the acceptance decisions, and estimate the model by maximizing a likelihood subject to a non-linear equilibrium constraint. The estimates reveal a substantial gap between preferences implicit in exposure and those governing acceptance. On the doctor side, conditional on being exposed to a selected post, acceptance is only weakly sensitive to post attributes; by contrast, the post side's acceptance remains selective even after exposure. At the individual variable level, the model captures disutility from distance: a 10% salary increase compensates for roughly a 5% decrease in distance for doctors and a 8% increase for posts at the exposure stage.

Based on the estimates, I compute the user–value–maximizing exposure rule and evaluate its implications. In the optimal exposure rule, the distance penalty largely disappears: exposure is nearly distance–neutral, in contrast to the baseline's clear decline with distance. As a metric of continuation values, I use the *log–salary offset*—the change in log salary that would offset the removal of continuation values from utility. In this measure, at the median, the salary offsets for doctors shifts from an

85% reduction to a 99% reduction, while for posts it rises from a 5% increase to a 23% increase. In other words, the computed exposure rule improves the user value on both sides relative to the realized platform. To diagnose where user value gain comes from, I also solve an exposure design problem in which each doctor's expected number of exposures is fixed to at its observed level. At that fixed scale, the optimal exposure does not exceed the realized market's user value. The reason is mechanical: in the realized market, exposure is chosen endogenously with respect to continuation values, so only sufficiently high–utility pairs are shown, which boosts user value even without explicitly optimizing the exposure rule. The broader lesson is that the number of exposures is first–order—expanding how many options users see generates the largest gains—while reweighting exposure delivers additional, but secondary, improvements once scale is held fixed.

Literature. This paper is closely related to the literature on sequential search in two-sided matching platforms. Adachi (2003) develops the canonical model and provides a microfoundation for the Gale–Shapley deferred-acceptance algorithm (Gale and Shapley, 1962): in the limit of vanishing search frictions, the equilibrium of two-sided sequential search converges to the Gale–Shapley outcome. The framework has been applied empirically; for example, Hitsch, Hortaçsu and Ariely (2010) study a dating platform, estimate participants' preferences using the Adachi (2003) model, and simulate market outcomes. An alternative equilibrium concept is the stable outcome of Shapley and Shubik (1971) for transferable-utility matching; Chen, Hsieh and Lin (2023) use this notion to construct a new recommendation algorithm improving matching quality in a dating service. However, these studies do not directly take the platform's objective as the object of optimization and thus provide limited validation from the platform's perspective. This paper fills that gap by explicitly formulating the platform's objective and proposing a tractable algorithm to solve for the exposure rule that maximizes it.

A growing literature in marketing/operations studies recommendation on multi-sided platforms with platform-level objectives beyond myopic clicks. Wang, Tao and Zhang (2025) develop a multi-objective hierarchical recommender tailored to two- (and three-)sided marketplaces, and document large-scale field deployment at Uber Eats with significant gains in conversion, retention, and gross bookings, while offering a principled way to trade off long- and short-run goals. Shi (2025) show that, despite price feedbacks, optimal policies admit a simple structure—effectively prioritizing providers with the highest price-adjusted conversion rates—and that ignoring price endogeneity can trap the market at strictly suboptimal equilibria. Relatedly, Shi (2023) study ε-stable outcomes in assignment games and design low-communication protocols that guarantee near–social-welfare optimality, connecting stability notions to implementable recommendation/matching procedures. Relative to these strands, my contribution is to make the platform's *dynamic* objective explicit: I formalize user value as the sum of continuation values in a two-sided sequential-search environment, quantify the wedge between user-value gradients and flow-match surplus, and compute exposure propensities that maximize user value. This brings the cannibalization channel into the optimization itself.

In computer science, another growing line of work makes the platform's objective explicit and optimizes it directly along three complementary fronts. First, the reinforcement learning strand learns policies for long-run engagement or value, using counterfactual objectives and doubly robust estimators, and scalable slate-value decompositions for large action spaces (Swaminathan and Joachims, 2015; Dudík, Langford and Li, 2011; Ie et al., 2019). Second, multi-objective and constraint-aware ranking

introduces provider or stakeholder constraints and fairness guarantees, often as post-processing or joint optimization over exposure subject to side constraints (Jambor and Wang, 2010; Sürer, Burke and Malthouse, 2018; Biega, Gummadi and Weikum, 2018). Third, differentiable assignment leverages entropically regularized optimal transport and continuous relaxations of sorting to enable end-to-end training with allocation decisions (Cuturi, 2013; Mena et al., 2018; Grover et al., 2019; Prillo and Eisenschlos, 2020). Most of these approaches rarely *internalize* how present exposure thins future option values through a general-equilibrium feedback. In contrast, our framework embeds the continuation values as an equilibrium object, thereby structurally capturing the cannibalization channel, while retaining computational tractability.

2 Model and Preliminary Results

I describe an online two-sided matching platform: following the empirical context discussed in Section 4, I consider a matching between doctors and spot job posts. Let I denote the set of active doctors, indexed by $i \in I$, and let J denote the set of spot posts, indexed by $j \in J$. At registration, the platform observes some covariates, but from the viewpoint of the other side each agent still has a latent "type" that is not initially observed. Because of this information friction, observed matches need not coincide with static equilibrium notions such as the stable outcome of Shapley and Shubik (1971).

I model the agent behavior as a two-sided sequential-search model like Adachi (2003). In this environment, private information is revealed upon "meeting," which can take several forms in practice such as direct messages or physical interview. After a meeting, the two parties decide whether to accept one another; a match forms only if both accept. If either side rejects, they separate and continue searching in the next period. A post typically takes from a few hours to several days, so it is natural that a doctor who matches with a post does not exit the platform unlike in the marriage market. Instead, the doctor soon returns and continues searching. On the post side, once a match with a doctor occurs, the post is permanently removed from the platform. But I assume a stationary environment in which similar posts are continuously supplied by similar institutions. This environment assures that the distribution of existing agent types is time-invariant.

I describe the model components in the following subsections. First, the individual decision problem: after a meeting and type revelation, each side either accepts the current counterparty or declines and continues searching. For this component, I mostly follow the formulation in Adachi (2003), with specifications tailored to my empirical application (Section 2.1). Second, the exposure rule: rather than assuming random encounters as in Adachi (2003), I allow the platform to design how agents are brought into meeting to pursue a platform objective. I also build a new system determining the continuation value of the agents in this platform (Section 2.2).

2.1 Agents' Decision Problem

I describe how agents on the platform act when meetings occur. Let α_i^D and α_j^P denote the *continuation values* for doctor i and post j who remain unmatched at the end of a period and continue searching. In this section they are taken as given; later they are determined as a model's solution.

Let U_{ij} denote the *matching utility* of doctor i from matching with post j after j's private type

is revealed. Because doctor i returns to the platform soon after completing the task at j, this utility decomposes into a *one-time* component, $\tilde{U}_{ij}$, and a discounted continuation value: $U_{ij} \equiv \tilde{U}_{ij} + (1-\kappa)\alpha_i^D$, where $1-\kappa$ captures the discount rate caused by the blank time spent on the post j.[1] The model primitive which is parameterized in my empirical application, is the *one-time matching utility* $\tilde{U}_{ij}$, not U_{ij}. Let V_{ji} denote the matching utility of post j from matching with doctor i after i's type is revealed. Since acceptance removes the post from the platform permanently, there is no continuation term on the post side; the model primitive is V_{ji} itself.

Doctor i accepts j iff $U_{ij} \geq \alpha_i^D$, and post j accepts i iff $V_{ji} \geq \alpha_j^P$. Equivalently, with acceptance indicators $a_{i,j}^D$ and $a_{j,i}^P$,

$$a_{i,j}^D \equiv \mathbf{1}\{U_{ij} \geq \alpha_i^D\} = \mathbf{1}\{\tilde{U}_{ij} \geq \kappa\alpha_i^D\}, \qquad a_{j,i}^P \equiv \mathbf{1}\{V_{ji} \geq \alpha_j^P\}. \tag{1}$$

Here, I implicitly assume a non-transferable-utility environment: matched pairs do not make side payments, and there is no ex post bargaining over contract terms.

For the empirical application below and the more concise expression, I assume that private types enter additively and are independently and identically distributed. Let $\tilde{U}_{ij}^{\text{det}}$ and V_{ji}^{det} denote the deterministic components, and let ε_{ij}^D and ε_{ji}^P denote the idiosyncratic private types.

Assumption 1. *(Additive and i.i.d. types) For all $i \in I\$and\$j \in J$,*

$$\tilde{U}_{ij} = \tilde{U}_{ij}^{\text{det}} + \varepsilon_{ij}^D, \qquad V_{ji} = V_{ji}^{\text{det}} + \varepsilon_{ji}^P,$$

where ε_{ij}^D and ε_{ji}^P are i.i.d. draws from a common distribution F, independent across pairs and across sides.

2.2 Exposure and Continuation Value

In a job matching platform, doctors and job posts each search for a match from the opposite side. To facilitate this process, the platform can introduce a set of *spot exposure rules*. A spot exposure rule provides agents on both sides with a set of suggested meetings with counterparts from the opposite side. In this article, I focus on the case where the platform can only use one-sided exposure rule and the exposure to the other side is determined by them. Specifically, the platform implements a spot exposure rule to the doctor side: it determines the set of posts exposed to each doctors. At the same time, the set of doctors exposed to a post is determined by a set of doctors exposed to the post. Hereafter, I define one *period* as a single instance of a spot exposure opportunity, and denote it by t when necessary.

A spot exposure rule is defined by specifying *spot exposure set* induced by it. Let $\tilde{R}_t$ denote a spot exposure set at a period t, which consists of two components—one for each side. I represent this as a tuple $\tilde{R}_t = (\tilde{R}_t^D, \tilde{R}_t^P)$, where D means the doctor side and P implies the post side. $\tilde{R}_t^D$ is a random variable taking values in $\left(2^J\right)^I$, and $\tilde{R}_t^P$ is a random variable taking values in $\left(2^I\right)^J$. Below I use subscript i and j to denote the spot exposure set of doctor and post: $\tilde{R}_{i,t}^D$ or $\tilde{R}_{j,t}^P$.

I introduce a tractable class of spot exposure rules indexed by an *exposure intensity* matrix $\mu = (\mu_{ij})_{i\in I, j\in J} \in [0,1]^{I\times J}$. Time is divided into sequences of J periods. At the beginning of each sequence,

[1] When $\kappa = 1$, the doctor's decision comes to whether to accept the post and exit from the market forever or to continue searching. This case corresponds to the marriage market analyzed in Adachi (2003); Hitsch, Hortaçsu and Ariely (2010); Chen, Hsieh and Lin (2023).

each doctor i draws a random permutation σ_i of J posts. In period $t \in \{1, \ldots, J\}$, the permutation selects a candidate post $j = \sigma_i(t)$. The platform then triggers an exposure between i and j with probability μ_{ij}, independently across doctors and periods. If the exposure is not triggered, doctor i receives no recommendation in that period. The exposure set on the post side is defined as the set of doctors who are exposed to that post in the same period. Formally, Definition 1 specifies the spot exposure set of i and j.

Definition 1 (Exposure sets induced by exposure intensity μ)**.** *Fix $\mu = (\mu_{ij})_{i\in I, j\in J} \in [0,1]^{I\times J}$. In each J-period sequence, every doctor i draws a permutation σ_i of J posts (independently across i), and in each period $t \in \{1, \ldots, J\}$ draws an exposure indicator*

$$X_{i,t} \sim \text{Bernoulli}\big(\mu_{i,\sigma_i(t)}\big),$$

independently across i and t conditional on $(\sigma_i)_i$. The spot exposure sets *are*

$$\tilde{R}^D_{i,t} := \begin{cases} \{\sigma_i(t)\}, & \text{if } X_{i,t} = 1, \\ \emptyset, & \text{if } X_{i,t} = 0, \end{cases} \qquad \tilde{R}^P_{j,t} := \{\, i \in I : \sigma_i(t) = j,\ X_{i,t} = 1 \,\}.$$

Doctor side I consider doctor i's dynamic decision in this platform. The flow utility obtained by remaining unmatch is normalized to 0. Under the assumption of additive separability (Assumption 1), following Adachi (2003), this dynamic decision problem is summarized by the following Bellman equation: where $\rho \in (0,1)$ is the discount factor and $\alpha^D_{i,t}$ and $\alpha^P_{j,t}$ are continuation values at t,

$$\alpha^D_{i,t} = \rho \int_{\varepsilon,\sigma,\tau} \left[\begin{array}{l} \mathbf{1}\{\tilde{R}^D_{i,t} = \emptyset\}\, \alpha^D_{i,t+1} \\ \quad + \sum_{j=1}^{J} \mathbf{1}\{j \in \tilde{R}^D_{i,t}\} \left\{ \begin{array}{l} \mathbf{1}\{V^{\text{det}}_{ji} + \varepsilon^P_{ji} > \alpha^P_{j,t}\}\, \max\{\tilde{U}^{\text{det}}_{ij} + (1-\kappa)\alpha^D_{i,t} + \varepsilon^D_{ij},\, \alpha^D_{i,t}\} \\ \quad + \mathbf{1}\{V^{\text{det}}_{ji} + \varepsilon^P_{ji} \le \alpha^P_{j,t}\}\, \alpha^D_{i,t} \end{array} \right\} \end{array} \right] \mathrm{d}F(\varepsilon,\sigma,\tau)$$

$$= \rho \int_{\varepsilon,\sigma,\tau} \left[\begin{array}{l} \mathbf{1}\{\tilde{R}^D_{i,t} = \emptyset\}\, \alpha^D_{i,t+1} \\ \quad + \sum_{j=1}^{J} \mathbf{1}\{j \in \tilde{R}^D_{i,t}\} \left\{ \alpha^D_{i,t} + \mathbf{1}\{V^{\text{det}}_{ji} + \varepsilon^P_{ji} > \alpha^P_{j,t}\}\, \max\{\tilde{U}^{\text{det}}_{ij} - \kappa\alpha^D_{i,t} + \varepsilon^D_{ij},\, 0\} \right\} \end{array} \right] \mathrm{d}F(\varepsilon,\sigma,\tau)$$

The probability that a post j is exposed at period t is simply $\frac{\mu_{ij}}{J}$.[2] Then, the Bellman equation is transformed into the following:

$$\alpha^D_{i,t} = \rho \left(1 - \sum_{j=1}^{J} \frac{\mu_{ij}}{J}\right) \alpha^D_{i,t+1} + \rho \sum_{j=1}^{J} \frac{\mu_{ij}}{J} W^D_{ijt},$$

[2] $\Pr\Big(j \in \tilde{R}^D_{i,t}\Big) = \Pr(\sigma_i(t) = j,\ X_{i,t} = 1) = \Pr(\sigma_i(t) = j)\Pr(X_{i,t} = 1 \mid \sigma_i(t) = j) = \frac{1}{J}\mu_{ij}$.

where

$$W_{ijt}^D \equiv \alpha_{i,t}^D + \int_\varepsilon \mathbf{1}\left\{V_{ji}^{det} + \varepsilon_{ji}^P > \alpha_{j,t}^P\right\} \max\{\tilde{U}_{ij}^{det} - \kappa\alpha_{i,t}^D + \varepsilon_{ij}^D,\, 0\} \mathrm{d}F(\varepsilon). \tag{2}$$

Post side I consider post j's dynamic decision. Again the flow utility of remaining unmatch is normalized to 0. Remark that the exposure set of post at period t is not always a singleton set. Let $u_j(S; \alpha_{j,t}^P, \alpha_t^D)$ denote the utility obtained when the exposure set is $S \in 2^I$. The Bellman equation of post side is written as follows:

$$\alpha_{j,t}^P = \rho \int_{\varepsilon,\sigma,\tau} \left[\mathbf{1}\left\{\emptyset = \tilde{R}_{j,t}^P\right\} \alpha_{j,t+1}^P + \sum_{S\in 2^I} \mathbf{1}\left\{S = \tilde{R}_{j,t}^P\right\} u_j\left(S; \alpha_{j,t}^P, \alpha_t^D\right) \right] \mathrm{d}F(\varepsilon,\sigma,\tau).$$

Instead of specifying $u_j(S; \alpha_{j,t}^P, \alpha_t^D)$, I put an assumption on the relative size of both sides to avoid the happenings of such multiple meeting. A necessary condition for S to be a non-singleton set is that $\sigma_i^A(t) = \sigma_{i'}^A(t)$ for at least one pair of i and i'. I call this incidence by *overlap*. Then, the probability of no overlap in a sequence, i.e. in J periods, is directly calculated as:

$$P_{I,J} = \Pr(\text{no overlap}) = \prod_{k=0}^{I-1}\Big(1 - \frac{k}{J}\Big).$$

By analyzing asymptotic behavior of this probability, I obtain the condition for no overlap in the large market.

Assumption 2. $I = o(\sqrt{J})$

Proposition 1. *Under Assumption 2, $P_{I,J} \to 1$ as $J \to \infty$.*

Proof. See Appendix A.1. □

Hence, under Assumption 2, when J is sufficiently large, the Bellman equation of post j is analogously as in the case of the doctor's Bellman equation: note that the probability of doctor i is exposed to post j at a period t is $\frac{\mu_{ij}}{J} \times \left(\frac{J-1}{J}\right)^{I-1}$ where the adjustment term $\left(\frac{J-1}{J}\right)^{I-1}$ captures the event that no other doctors are never exposed to j at the period[3],

$$\alpha_{jt}^P = \rho\left(1 - \sum_{i=1}^I \frac{\mu_{ij}}{J}\left(\frac{J-1}{J}\right)^{I-1}\right)\alpha_{jt+1}^P + \rho\left(\frac{J-1}{J}\right)^{I-1}\sum_{i=1}^I \frac{\mu_{ij}}{J} W_{ijt}^P,$$

where

$$W_{ijt}^P \equiv \alpha_{j,t}^P + \int_\varepsilon \mathbf{1}\left\{\tilde{U}_{ij}^{det} + \varepsilon_{ij}^D > \kappa\alpha_{i,t}^D\right\} \max\{V_{ji} - \alpha_{j,t}^P + \varepsilon_{ji}^P, 0\} \mathrm{d}F(\varepsilon). \tag{3}$$

Stationary solution Under Assumption 1 and 2, when the number of posts is sufficiently large, the system determining the continuation values of doctors and posts under the spot exposure rule induced by

[3]You can find that $\sum_i \frac{\mu_{ij}}{J} \times \left(\frac{J-1}{J}\right)^{I-1} \le \sum_i \frac{1}{J} \times \left(\frac{J-1}{J}\right)^{I-1} = {}_IC_1 \frac{1}{J}\left(\frac{J-1}{J}\right)^{I-1} \le 1$.

an exposure intensity is as follows: where W^D and W^P are defined as in (2) and (3), and $\tau \equiv \left(\frac{J-1}{J}\right)^{I-1}$,

$$\begin{cases} \alpha^D_{i,t} = \rho\left(1 - \sum_{j=1}^{J} \frac{\mu_{ij}}{J}\right)\alpha^D_{i,t+1} + \rho\sum_{j=1}^{J} \frac{\mu_{ij}}{J} W^D_{ijt}, \\ \alpha^P_{jt} = \rho\left(1 - \sum_{i=1}^{I} \frac{\mu_{ij}}{J}\tau\right)\alpha^P_{jt+1} + \rho\tau\sum_{i=1}^{I} \frac{\mu_{ij}}{J} W^P_{ijt}. \end{cases} \tag{4}$$

Hereafter, I use α to denote the vector of continuation values stacking the values of both sides. Note that period t only exists in α's subscript in the above system. This implies that, for some map g, I can write $\alpha_{t+1} = g(\alpha_t)$ for all $t = 1, \cdots, J$. Then, because another J periods begins after one sequence of J periods, $\alpha_1 = g(\alpha_J) = g(g(\alpha_{J-1})) = g^J(\alpha_1)$ where g^J denotes the J-fold composition of g. This argument can be applied to all t: for all the t, $\alpha_t = g^J(\alpha_t)$. This statement implies that the continuation values are periodic solution, or the stationary solution as a special case, of the system.

Theorem 1 establishes that the system g has a unique stationary solution under suitable regularity conditions. The result follows from a Lipschitz bound for g derived in Lemma 1 in Appendix A.2. In Example 1, I show a specific sufficient condition for this result when the private types ε follow a unit-scale type I extreme value distribution, which is assumed in the later empirical application. Furthermore, I show how easily the sufficient condition for the contraction mapping is satisfied in the case of the extreme value distribution, particularly when J and I are large.

Theorem 1 (Stationary uniqueness via contraction)**.** *Assume the conditions of Lemma 1 and let R and $q_R^{(\kappa)}$ be as defined there. If $q_R^{(\kappa)} < 1$, then:*

1. *(*Existence & Uniqueness*) There exists a unique stationary solution $\alpha^\star \in B_R$ to the system $\alpha^\star = g(\alpha^\star)$.*
2. *(*Global convergence*) For any initial $\alpha^{(0)} \in B_R$, the iteration $\alpha^{(k+1)} = g(\alpha^{(k)})$ converges to $\alpha^\star$ at a linear rate bounded by $\left(q_R^{(\kappa)}\right)^k$ under the sup norm.*
3. *(*No nonstationary cycles*) If $g^k(\alpha) = \alpha$ for some $k \geq 1$, then necessarily $\alpha = \alpha^\star$. In particular, no nontrivial periodic orbits exist.*

Proof. By Lemma 1, g is a contraction on the complete metric space $(B_R, \|\cdot\|_\infty)$ with modulus $q_R^{(\kappa)} < 1$. Banach's fixed point theorem yields (1) and (2). For (3), if $g^k(\alpha) = \alpha$ then

$$\|\alpha - \alpha^\star\|_\infty = \|g^k(\alpha) - g^k(\alpha^\star)\|_\infty \leq \left(q_R^{(\kappa)}\right)^k \|\alpha - \alpha^\star\|_\infty,$$

hence $\alpha = \alpha^\star$. □

Example 1 (Type I extreme value shocks)**.** *Assume the conditions of Lemma 1 under the Bernoulli exposure rule. In addition, suppose $\varepsilon^D, \varepsilon^P$ are independent Type I extreme value shocks (unit scale), and $\tilde{U}_{ij}^{\text{det}}, V_{ji}^{\text{det}} \in [0,1]$ for all (i,j). Let*

$$m_1 \;:=\; \mathbb{E}[|\varepsilon|] \;=\; \sqrt{\tfrac{\pi^2}{6} + \gamma^2} \qquad (\gamma \textit{ Euler's constant}), \qquad C_0 \;:=\; 1 + m_1,$$

so that $C_D^{(\kappa)} \leq C_0$ and $C_P \leq C_0$ for all $\kappa \in (0,1]$. Moreover, the unit-scale Type I extreme value density satisfies $\sup_x f(x) = 1/e$.

Define

$$\gamma^D_{\max} := \max_i \frac{1}{J}\sum_{j\in J}\mu_{ij}, \qquad \gamma^P_{\max} := \max_j \tau\,\frac{1}{J}\sum_{i\in I}\mu_{ij}, \qquad \tau := \left(\tfrac{J-1}{J}\right)^{I-1}.$$

Take

$$R \;=\; \frac{\rho}{1-\rho}\,C_0\,\max\{\gamma^D_{\max},\gamma^P_{\max}\}.$$

Then the Lipschitz modulus in Lemma 1 satisfies the bound

$$q_R^{(\kappa)} \;\le\; \rho\,\max\{\gamma^D_{\max},\gamma^P_{\max}\}\left[1+\frac{C_0}{e}\left(1+\frac{\rho}{1-\rho}\max\{\gamma^D_{\max},\gamma^P_{\max}\}\right)\right].$$

In particular, a simple sufficient condition for $q_R^{(\kappa)} < 1$ is

$$\rho\,\max\{\gamma^D_{\max},\gamma^P_{\max}\}\left[1+\frac{C_0}{e}\left(1+\frac{\rho}{1-\rho}\max\{\gamma^D_{\max},\gamma^P_{\max}\}\right)\right] \;<\; 1.$$

This sufficient condition is easy to satisfy in large markets. First, the doctor-side exposure mass $\gamma^D_{\max}$ is at most 1 and is often much smaller when each doctor is shown only a small fraction of posts on average. Second, the post-side term $\gamma^P_{\max}$ is multiplied by $\tau = ((J-1)/J)^{I-1} \approx \exp(-(I-1)/J)$, which decays rapidly when I is large relative to J, making the post-side contribution negligible. Thus, even for fairly high ρ, moderate J together with large I typically implies $q_R^{(\kappa)} < 1$.

The stationary version of the system (4) is written as follows:

$$\begin{cases} \alpha^D_i = \frac{\rho}{1-\rho}\sum_{j=1}^{J}\frac{\mu_{ij}}{J}\int_\varepsilon \mathbf{1}\left\{V^{det}_{ji}+\varepsilon^P_{ji} > \alpha^P_j\right\}\max\{\tilde{U}^{det}_{ij}-\kappa\alpha^D_i+\varepsilon^D_{ij},\,0\}\mathrm{d}F(\varepsilon), \\ \alpha^P_j = \frac{\rho\tau}{1-\rho}\sum_{i=1}^{I}\frac{\mu_{ij}}{J}\int_\varepsilon \mathbf{1}\left\{\tilde{U}^{det}_{ij}+\varepsilon^D_{ij} > \kappa\alpha^D_i\right\}\max\{V_{ji}-\alpha^P_j+\varepsilon^P_{ji},0\}\mathrm{d}F(\varepsilon). \end{cases} \tag{5}$$

The solution of system (5) is interpreted as an *equilibrium* of the two-sided sequential search model (Adachi, 2003; Hitsch, Hortaçsu and Ariely, 2010). In other words, doctors decide whether to accept or reject the exposed post based on their continuation values, thereby creating match opportunities for the post side, which likewise decides based on its continuation values (and vice versa). Furthermore, as shown in Theorem 1, this equilibrium is unique under suitable regularity conditions, which paves the way for the empirical application. Hereafter, I only consider the system (5), which is expressed as $\alpha = g(\alpha,\mu)$. I use $\alpha^D(\mu)$ and $\alpha^P(\mu)$ to denote the stationary solution of the system.

In this stationary environment the distribution of doctors and posts is constant. What changes by different exposure rule is the effective options faced by those who remain unmatched. An exposure rule that rushes the "best pairs" together skims off the mutually attractive encounters as soon as they arrive. Conditional on not having matched in the current period, an agent's subsequent exposures become systematically worse along two margins: (i) the counterparts she meets are, on average, less appealing to her; and (ii) conditional on meeting, she is less appealing to them, so acceptance from the other side is less likely. These are policy–induced shifts in the composition of meetings, not a change in the population itself. Because continuation values are the expected gains from future exposures, these shifts depress continuation values even though the platform is stationary in levels. This is the sense in which the "market thins" in our model: not fewer people, but worse prospects for the agents who still need another draw.

3 Exposure Design

I formulate the platform's exposure-design problem where I restrict attention to exposure rules induced by an exposure intensity; thus, the optimal exposure rule is the one induced by the optimal intensity. First, in Section 3.1, building on the system that governs agents' behavior on the platform, I introduce *user value*, defined as the sum of continuation values, as a objective function of the platform in comparison with aggregate flow match surplus. In Section 3.2, I present a tractable algorithm to compute the exposure intensity that maximizes user value.

3.1 Match Surplus and User Value

I take the equilibrium continuation values as the core of the platform's objective. This choice reflects that platforms seek to grow and retain their user base, and participation hinges on the perceived value of staying—naturally captured by continuation values. Yet it is not obvious which exposure rule maximizes user value, defined as the sum of continuation values, because the platform must trade off two opposing forces: raising contemporaneous match quality versus thinning the future options of those who remain unmatched. Below, I make this trade-off explicit and show that the exposure rule that maximizes aggregate *flow* match surplus generally differs from the rule that maximizes user value.

For a formal discussion, let $\mathcal{B}$ denote the budget polytope:

$$\mathcal{B} = \left\{ \mu \in [0,1]^{I \times J} : \; l_i^r \le \textstyle\sum_j \mu_{ij} \le c_i^r, \quad l_j^c \le \textstyle\sum_i \mu_{ij} \le c_j^c \right\}.$$

In this set, the row sums $\sum_j \iota_{ij}$ and column sums $\sum_i \iota_{ij}$—the expected numbers of exposures for doctor i and for post j in a single sequence of J periods—are bounded below by $l_i^r \in \mathbb{R}_+$ and $l_j^c \in \mathbb{R}_+$ and above by $c_i^r \in \mathbb{R}_+$ and $c_j^c \in \mathbb{R}_+$. For any $\mu \in \mathcal{B}$, I define the *aggregate flow match surplus*, $S(\mu)$, and the *user value*, $U(\mu)$, by

$$S(\mu) \equiv \frac{1}{J} \sum_{i,j} \mu_{ij} W_{ij}^D + \frac{\tau}{J} \sum_{i,j} \mu_{ij} W_{ij}^P, \qquad U(\mu) \equiv \frac{1}{\rho} \left(\sum_i \alpha_i^D + \sum_j \alpha_j^P \right).$$

Note that these values are *per-arrival* value in the sense that these values multiplied by ρ are contributions to the current continuation values as shown in system (4).

Proposition 2 establishes a wedge between the platform's aggregate flow match surplus $S(\mu)$ and the long-run user value $U(\mu)$: maximizing $S(\mu)$ need not maximize $U(\mu)$. Moreover, at any interior maximizer of S, the user-value gradient is componentwise nonnegative whenever the associated adjoint vector is nonnegative. Proposition 5 in Appendix A.4 provides a sufficient condition for this adjoint nonnegativity under the EV1 specification, and shows that the condition becomes mild in large markets. Taken together, these results imply that the S-optimal exposure intensity typically understates user value: from the perspective of maximizing U, the optimal rule tends to under-expose pairs.

Proposition 2 (Flow optimum induces nonnegative user-gradient)**.** *Fix $\mu \in \mathcal{B}$ and let $\alpha(\mu) = (\alpha^D(\mu), \alpha^P(\mu))$ be the unique stationary solution of the fixed-point system $G(\alpha, \mu) \equiv \alpha - g(\alpha, \mu) = 0$. Let $\mu^\star_{\text{flow}}$ be an interior maximizer of $S(\mu)$, so that $\nabla_\mu S(\mu^\star_{\text{flow}}) = 0$. If the associated adjoint vector π is componentwise*

nonnegative, then

$$\nabla_\mu U(\mu^\star_{\text{flow}})_{ij} \;\geq\; 0 \qquad \textit{for all } (i,j),$$

where $\pi = (\pi^D, \pi^P) \in \mathbb{R}^{I+J}$ *solves the adjoint linear system*

$$M^\top \pi \;=\; (\mathbf{1}_I, \mathbf{1}_J)^\top, \qquad M \equiv \frac{\partial G}{\partial \alpha}(\alpha, \mu^\star_{\text{flow}}) \in \mathbb{R}^{(I+J)\times(I+J)}.$$

Proof. See Appendix A.3. □

3.2 Exposure Design for User Value Maximization

The platform's problem is defined as follows:

$$\textbf{(P)} \quad \Big| \max_{\mu \in \mathcal{B}} \quad \sum_i \alpha_i^D(\mu) + \sum_j \alpha_j^P(\mu).$$

P is a constrained optimization over $I \times J$ variables subject to the nonlinear fixed-point constraints in (4). It is difficult to solve—and in practice often numerically unstable—especially in large markets. Furthermore, if there are multiple maximizers of **P**, I cannot set a strict rule on which one is chosen.

To avoid these issues, I reformulate **P** into a more tractable and numerically stable problem by introducing an entropic regularization. The objective value of **P** is recovered as the zero–temperature limit of the entropically regularized problem. Furthermore, when **P** has multiple maximizers, the zero-temperature limit selects the one that is KL–closest to a baseline exposure.

3.2.1 Regularized Problem

Let $\varepsilon > 0$ be a *temperature parameter* and let q be a strictly positive *baseline exposure* that lies in the interior of the budget polytope. An entropic regularization of **P** is defined as follows:

$$(\mathrm{P}_\varepsilon) \quad \Big| \max_{\mu \in \mathcal{B}} \quad \sum_i \alpha_i^D(\mu) + \sum_j \alpha_j^P(\mu) - \varepsilon \sum_{ij} \mu_{ij} \ln \frac{\mu_{ij}}{q_{ij}},$$

where the last term represents a KL divergence between μ and q: and so I denote the term by $\mathrm{KL}(\mu\|q) \equiv \sum_{i,j} \mu_{ij} \ln \frac{\mu_{ij}}{q_{ij}}$.

3.2.2 Zero-temperature Limit

I propose the zero-temperature limit of the solution of (P_ε) as a solution of the original platform problem **P**. It is natural to think the solution of this regularized problem converges to the solution of the original problem in some as $\varepsilon \downarrow 0$. Theorem 2 formalizes this correspondence and shows how the limit solution is selected from a possibly multiple solutions of **P**.

Theorem 2 (Zero-temperature limit)**.** *For* $\varepsilon > 0$ *and* $q_{ij} \in \mathcal{B}$*, define the regularized objective*

$$\Phi_\varepsilon(\mu) := U(\mu) - \varepsilon\, \mathrm{KL}(\mu\|q), \qquad \mathrm{KL}(\mu\|q) = \sum_{ij} \mu_{ij} \ln \frac{\mu_{ij}}{q_{ij}}.$$

Let $\mu_\varepsilon \in \arg\max_{\mu \in \mathcal{B}} \Phi_\varepsilon(\mu)$*. Then:*

(i) *Every limit point* μ^0 *of* $\{\mu_\varepsilon\}_{\varepsilon \downarrow 0}$ *satisfies* $U(\mu^0) = \max_{\mu \in \mathcal{B}} U(\mu)$.

(ii) *Let* $\mathcal{M} := \arg\max_{\mu\in\mathcal{B}} U(\mu)$. *Every limit point* μ^0 *lies in* $\mathcal{M}$ *and minimizes KL on* $\mathcal{M}$*: i.e.,* $\mu^0 \in \arg\min_{\mu\in\mathcal{M}} \mathrm{KL}(\mu\|q)$. *If this minimizer is unique, then* $\mu_\varepsilon \to \mu^0$.

Proof. For any $\mu^\star \in \arg\max U$, optimality of μ_ε gives

$$U(\mu_\varepsilon) - \varepsilon\,\mathrm{KL}(\mu_\varepsilon\|q) \;\geq\; U(\mu^\star) - \varepsilon\,\mathrm{KL}(\mu^\star\|q).$$

Thus $U(\mu_\varepsilon) \geq U(\mu^\star) - \varepsilon\,\mathrm{KL}(\mu^\star\|q)$, so $U(\mu_\varepsilon) \to \max_\mu U(\mu)$. By compactness of $\mathcal{B}$, any limit point μ^0 satisfies $U(\mu^0) = \max_\mu U(\mu)$, proving (i).

For (ii), for any $\mu \in \mathcal{M}$ the same inequality rearranges to

$$\mathrm{KL}(\mu_\varepsilon\|q) \;\leq\; \mathrm{KL}(\mu\|q) \;+\; \frac{U(\mu_\varepsilon) - U(\mu)}{\varepsilon}.$$

Since $U(\mu_\varepsilon) \to U(\mu)$ for all $\mu \in \mathcal{M}$, the last term vanishes in the limit. By lower semicontinuity of KL, $\mathrm{KL}(\mu^0\|q) \leq \liminf_{\varepsilon\downarrow 0} \mathrm{KL}(\mu_\varepsilon\|q) \leq \mathrm{KL}(\mu\|q)$ for all $\mu \in \mathcal{M}$, so μ^0 is a KL minimizer on $\mathcal{M}$. Uniqueness of this minimizer implies full convergence. □

3.3 Algorithm

For a fixed $\varepsilon > 0$, problem P_ε is a KL-regularized optimization problem over the convex feasible set $\mathcal{B}$.[4] Rather than using the standard Sinkhorn algorithm, which is tailored to simple marginal constraints, we solve P_ε via the Bregman–Dykstra iterative projection method (Benamou et al., 2014). This method generalizes Sinkhorn to an intersection of convex constraints and produces iterates that remain feasible with respect to $\mathcal{B}$.

To approximate the zero-temperature limit, we employ an annealing scheme in which the temperature is gradually reduced, $\varepsilon \downarrow 0$. At each temperature level, we run the Bregman–Dykstra iterations to convergence and use the resulting solution to warm-start the next temperature. Pseudocode is provided in Algorithm 1.

4 Empirical Application

I apply the model to a doctor-spot post matching platform and compute the optimal exposure rule. In Section 4.1, I introduce the background information of this platform and show a set of descriptive statistics to gauge the whole picture. In Section 4.2, I specify the data generating process and how to parametrize the model primitives to identify the model. In Section 4.3, I show the estimation results and gives some insights into the agent's decisions in this platform. Lastly, in Section 4.4, I apply Algorithm 1 to this situation and compare the results to the other exposure rules.

4.1 Institutional Background and Data

The empirical setting is a two-sided platform that matches doctors to short-term "spot" posts, operated by Medical Principle Co. in Japan. The platform is part of the firm's broader medical-staffing business. It serves doctors who already hold a medical license and have completed their internship—typically

[4] Equivalently, it can be viewed as an entropically regularized problem with a reference point q, subject to convex constraints.

Table 1. Mapping from Approach Status to Accept Indicators

	Approach Status				
	Contract	Cancelled After Contract	NotHired	Approach	Inquiry Handled
doctor accept	1	1	1	0	0
post accept	1	1	0	1	-

Notes: 1 = accept, 0 = reject, - = not defined.

physicians who maintain a full-time position at a medical institution. On the demand side, hospitals and clinics contract with Medical Principle and list short-term openings at their facilities on the website, and the platform intermediates applications and selection between doctors and providers.

I start by describing the detail of this platform. On the doctor side, doctors can search the website to find suitable posts. Medical institutions do not directly search for candidates; instead, *agents* at Medical Principle curate promising doctors from the platform's user base, facilitating matches. The contents of spot posts vary widely—e.g., overnight on-call shifts, health checkups, and ward coverage—and range from a few hours or a single day to, in some cases, about a week. Doctors remain on the platform after each match and—after an interval that differs across individuals—often return to take additional spot work. By contrast, a task leaves the market once it is filled; yet many categories such as overnight duty recur frequently as similar tasks, so the inflow into the platform is stationary.

I now describe the sequence in which a vacancy is filled on the platform. First, an "approach" between a doctor and a post is generated either by the doctor's web search or by a curated introduction from Medical Principle's agents; in the data we observe both the occurrence of an approach and its channel. This approach corresponds with the meeting in my model. Once an approach occurs, the pair enters an information-exchange stage in which detailed attributes and terms are disclosed—typically via inquiries routed through Medical Principle, and occasionally supplemented by an in-person or online interview. Given this additional information, each side decides whether to accept or decline the current counterpart; a match is formed only under bilateral acceptance. Importantly, even when a doctor initiated the approach through search, the doctor may later decline after learning more: for example, the workload proves demanding, the location is less accessible, and scheduling is inconvenient. Symmetrically, post-side declines are also common.

For each approached pair, I also observe whether each side accepted or declined the counterpart. This is because the platform records an "approach status" for every pair—one of *Contract*, *Cancelled After Contract*, *Not Hired*, *Approach*, or *Inquiry Handled*. Using this status, we define binary indicators of doctor- and post-side acceptance as in Table 1. For example, *Contract* implies mutual acceptance, whereas *Not Hired* indicates that only the doctor accepted the post. The mapping was constructed in consultation with Medical Principle's staff. This information allows me to infer the outcome of post-approach decisions from observed statuses.

In addition to the behavioral histories, the platform records rich attributes for each participant. On the doctor side, available fields include age, years since licensure, medical specialty, home address, and preferred task content. On the post side, the record includes the latitude–longitude of the work site, task content, desired doctor specialty, working hours, and compensation. For task content, providers select from predefined pull-down categories but may also supply free-text descriptions; further details are often revealed through direct inquiries. In our model, such information beyond the observed covariates affects

Table 2. Market size and acceptance patterns by exposure rule

Panel A: Market size and outcomes					
Number of posts (J)					2,446
Number of doctors (I)					1,132
Number of approaches					3,898
Number of agreed contracts					1,358
Agreement rate (overall)					34.84%
Panel B: Approaches per entity					
	Mean	*SD*	*Min*	*Median*	*Max*
Per post	1.594	1.527	1	1	23
Per doctor	3.443	4.474	1	2	46
Panel C: Acceptance by exposure rule					
				Agency (A)	*Self-search (S)*
Share of approaches				30.20%	69.80%
Doctor accepts				30.80%	97.95%
Post accepts				97.75%	40.64%
Both accept (contract)				28.58%	40.64%

Notes: Shares and rates are computed over observed approaches. The overall agreement rate equals agreed contracts divided by approaches (1358/3898 = 34.84%).

payoffs and is treated as private information realized at the time of a meeting.

Finally, I outline the business model and the competitive environment. Medical Principle operates in a competitive, non-exclusive market: several comparable platforms exist in Japan, and both doctors and facilities commonly multi-home. Doctors use the service free of charge, whereas facilities pay listing fees to post vacancies. Profit maximization thus works through reinforcing cross-side network effects: posting more and more attractive vacancies increases the platform's value to doctors; a larger, more engaged doctor base, in turn, raises the platform's value to facilities and their willingness to pay for listings. In this sense, given the number of participants, MD's objective can be viewed as maximizing the user value which the current participants feel in the platform and surely affects the entry decision of the potential users.

Descriptive Statistics I fix the sets of doctors I and posts J as follows: I consists of doctors who are exposed to at least one approach in *December 2024*, and J consists of posts that are exposed to at least one approach in the same month. This restriction is necessary because many doctors and posts are idle; I therefore focus on the participants that conduct some form of active decision. Furthermore, I restrict the posts open in Kanto region in Japan.

Table 2 summarizes the descriptive stats about the market size and acceptance patterns. The December market comprises 2,446 posts and 1,132 doctors with 3,898 observed approaches, yielding 1,358 agreed contracts (overall agreement rate: 34.8%). Approaches are sparse on the post side and more dispersed across doctors, suggesting a long right tail of highly active doctors. Self-search accounts for roughly 70% of approaches. Acceptance patterns differ sharply by exposure rule: under self-search, doctors almost always accept (98.0%) while posts are selective (40.6%); under agency recommendations, posts almost always accept (97.8%) but doctors are selective (30.8%). The contract rate is higher for self-search (40.6%) than for agency (28.6%), despite the latter's very high post acceptance.

Table 3 reports summary statistics for doctor- and post-level variables. Panel A shows doctors are

Table 3. Descriptive statistics of doctor-level and post-level variables

Panel A: Doctor-level (N = 1,132)					
Variable	Mean	SD	Min	Median	Max
Age	42.7	12.1	27.0	40.0	79.0
Exp (yrs)	16.5	11.8	2.00	13.0	53.0
Panel B: Post-level (N = 2,446)					
Variable	Mean	SD	Min	Median	Max
Hours	10.0	8.66	0.500	8.50	114
Pay (×1k yen)	72.1	43.4	4.00	60.0	650
Wage/hr	9.25	4.18	0.833	10.0	56.8

Notes: *Wage/hr* = *Pay/hours*. All figures rounded to three significant digits.

on average 42.7 years old with 16.5 years of experience. This implies that they are mature doctors and their skills are not in severe doubt unlike early-career doctors. Panel B summarizes post side: shifts average 10.0 hours, advertised pay averages 72.1 thousand yen, and the implied hourly wage averages 9.25 thousand yen.[5] The wide ranges and gaps between means and medians indicate substantial heterogeneity in workload and compensation across posts.

In addition to the variables in Table 3, the dataset includes each doctor's specialty and, for each post, the desired doctor specialties. Figure E.1 shows the distribution of doctors across specialties. Most posts specify two desired specialties—a primary and a secondary. Figure E.2 reports the number of posts that list each specialty as the primary one. In both sides of the market, internal medicine is the most prevalent specialty; roughly 50% of posts list internal medicine as their primary specialty. This pattern is consistent with the nature of spot work: internal medicine is often bundled with routine services such as general health checkups, which are well suited to short-term shifts. By contrast, specialties that involve highly specialized tasks (e.g., cardiology) generate far fewer posts. On the supply side, however, doctors' registered specialties are less skewed, because physicians with specialized training can still perform routine checkups; consequently, the distribution across doctors is more dispersed than the distribution of posts.

Lastly, I present descriptive statistics for pairwise doctor–post variables. For each post's primary–secondary specialty pair, the platform specifies the set of doctor specialties that can "match" the post; this indicator serves as a criterion in the agency recommendation. Figure E.3 reports the average number of posts matched to each doctor specialty; as expected, internal medicine affords the most opportunities. Although this match indicator is not a binding constraint on realized matches, it is included as a covariate in the empirical analysis below. The mean doctor–post distance is 62.0km (median 353,km). In the Kanto region, where rail is the primary mode of transport, such distances correspond roughly to 30–60 minutes of travel time.

4.2 Empirical Strategy

The platform implements two exposure rules: *self-search exposure* (S) and *agency-recommendation exposure* (A). They are specified formally later. I observe the exposure sets generated by each rule; let

[5] Using the USD/JPY spot rate of 147.85 on September 12, 2025, 72.1 thousand yen ≈ \$488 and 9.25 thousand yen ≈ \$62.6.

$k \in \{S, A\}$ index the rule and the exposure sets are denoted by $C^D_{k,i} \in 2^J$ for doctors. These sets are *disjoint*: for any pair (i, j), the data specify at most one rule under which i and j are exposed to each other. Define inclusion indicators for the exposure sets as follows: for each pair (i, j), $c^D_{k,i,j} \equiv \mathbf{1}\{\, j \in C^D_{k,i} \,\}$. Note that the exposure set of post is automatically determined by these doctor side exposure sets. For the meeting pairs, I also observe the acceptance decisions of both sides. Remember that these are denoted by $a^D_{i,j}$ and $a^P_{j,i}$. When a pair (i, j) does not meet, these indicators take a null value ϕ. In short, an "outcome variable" of one data point (i, j) is $y_{ij} \equiv \big(a^D_{i,j}, a^P_{j,i}, (c^D_{S,i,j}, c^D_{A,i,j})\big)$.

In the data-generating process, y_{ij} is produced over J periods of spot-exposure rules corresponding to the two rules and agents' decisions after each meeting. A spot exposure rule, $k \in \{A, S\}$ is an exposure rule whose pairwise exposure intensity is denoted by μ^k_{ij}. At each period t, the random permutation, σ^k_i, determines a possible counterpart and, the counterpart is drawn from a Bernoulli distrbituon with parameter μ^k_{ij}, there is an exposure between j and j. The two spot exposure rules function independently, and the exposure label for a pair is determined by whichever rule triggers exposure first. If both of the spot exposure rules draw the same counterpart at the same period, I assume that S is prioritized.

I can calculate the probability of an observation y_{ij} by

$$\Pr(y_{ij}) = \Pr\big(a^D_{i,j},\, a^P_{j,i} \mid c^D_{S,i,j},\, c^D_{A,i,j}\big) \cdot \Pr\big(c^D_{S,i,j},\, c^D_{A,i,j}\big)\,.$$

The first term follows from the distribution of private types due to Definition 1 under Assumption 1. For the second term, the probabilities of the exposure-indicator pair $(c^D_{S,i,j}, c^D_{A,i,j})$ can be written as functions of the pairwise exposure intensities μ^S and μ^A. Proposition 3 summarizes the expressions for the three mutually exclusive cases: $(1, 0)$, $(0, 1)$, and $(0, 0)$.

Proposition 3.

$$\Pr\big((c^D_{S,i,j}, c^D_{A,i,j}) = (1,0)\big) = \mu^S_{ij}\left(1 - \frac{J-1}{2J}\,\mu^A_{ij}\right),$$

$$\Pr\big((c^D_{S,i,j}, c^D_{A,i,j}) = (0,1)\big) = \mu^A_{ij}\left(1 - \frac{J+1}{2J}\,\mu^S_{ij}\right),$$

$$\Pr\big((c^D_{S,i,j}, c^D_{A,i,j}) = (0,0)\big) = (1-\mu^S_{ij})(1-\mu^A_{ij}).$$

Proof. See Appendix A.5 □

Therefore, in the empirical analysis that follows, I parameterize the distribution of the acceptance indicators and the two pairwise exposure intensities. Section 4.2.1 introduces logit-form parameterizations for all required components, and Section 4.2.2 constructs the likelihood accordingly. Because the exposure rules depend on agents' continuation values as clarified later, the likelihood is subject to nonlinear equilibrium constraints that pin down those continuation values. Lastly, in Section 4.2.3, I provide the detail of the estimation of the model: I estimate the model using a nested fixed-point algorithm (Rust, 1987).

4.2.1 Parametrization

I parametrize the preference structure of the agents in this platform and specify the acceptance indicators. For each doctor–post pair (i, j), let X_{ij} denote observable characteristics which are known to the platform

operator, all agents, and the researcher. X_{ij} form the deterministic component of the (one-time) matching utilities, $\tilde{U}_{ij}^{det}$ and V_{ji}^{det}, as follows:

$$\tilde{U}_{ij}^{det} = X_{ij}'\beta^D + Z_{ij}'\delta^D, \quad V_{ji} = X_{ij}'\beta^P + Z_{ij}'\delta^P,$$

where Z_{ij} is a set of polynomials of X_{ij} which captures the *non-linear terms* in the preferences. For now, I fix the continuation values α_i^D and α_j^P. Then, under Assumption 1, the acceptance indicators $a_{i,j}^D$ and $a_{j,i}^P$, which are defined in (1), is specified as follows: for each meeting pair (i,j),

$$a_{i,j}^D = \begin{cases} 1 & \text{if } X_{ij}'\beta^D + Z_{ij}'\delta^D + \varepsilon_{ij}^D > \kappa\alpha_i^D \\ 0 & \text{otherwise} \end{cases}, \quad a_{j,i}^P = \begin{cases} 1 & \text{if } X_{ij}'\beta^P + Z_{ij}'\delta^P + \varepsilon_{ij}^P > \alpha_j^P \\ 0 & \text{otherwise} \end{cases},$$

I use $\theta_{\text{pref}} \equiv \left(\beta^D, \beta^P, \delta^D, \delta^P\right)$ to denote the set of preference parameters. The doctor-side private type ε_{ij}^D is i.i.d. across pairs with distribution H^D, and the post-side private type ε_{ji}^P is i.i.d. across pairs with distribution H^P. We assume that H^D and H^P are logistic distributions with scale parameters ζ^D and ζ^P, respectively. The acceptance probabilities for the two sides, denoted P_{ij}^D and P_{ji}^P, are given by:

$$P_{ij}^D \equiv \Pr\left(a_{i,j}^D = 1\right) = \frac{1}{1 + \exp\left(\frac{\kappa\alpha_i^D - X_{ij}'\beta^D + Z_{ij}'\delta^D}{\zeta^D}\right)}, \quad P_{ji}^P \equiv \Pr\left(a_{j,i}^P = 1\right) = \frac{1}{1 + \exp\left(\frac{\alpha_j^P - X_{ij}'\beta^P + Z_{ij}'\delta^P}{\zeta^P}\right)}.$$

Remember that there are two exposure rules. Below, I formally specify how these rules operate. For now, I fix the continuation values α_i^D and α_j^P.

Self-search exposure. This exposure rule functions by repeating a J-period sequence. The spot-exposure sets for doctor i and post j are defined as follows:

$$\begin{cases} \tilde{R}_{S,i,t}^D &= \left\{j \in J \mid \sigma_i^S(t) = j, X_{ij}'\beta^D + Z_{ij}'\delta^S + \tilde{v}_{ijt}^S > \kappa\alpha_i^D + \tilde{v}_{ijt0}^S\right\} \\ \tilde{R}_{S,j,t}^P &= \left\{i \in I \mid \sigma_i^S(t) = j, X_{ij}'\beta^D + Z_{ij}'\delta^S + \tilde{v}_{ijt}^S > \kappa\alpha_i^D + \tilde{v}_{ijt0}^S\right\}, \end{cases}$$

where the difference between δ^S and δ^D, which appears in doctor's preference, captures a kind of *mis-perception*: after meeting the doctor's preference might be altered. σ_i^S is a random permutation of $\{1, \ldots, J\}$. $(\tilde{v}_{ijt}^S, \tilde{v}_{ijt0}^S)$ are idiosyncratic errors in the perceived utility that are not accounted for by the deterministic components. The distribution of them is denoted H^S. I assume that H^S is a type-I extreme-value distribution with scale parameter ζ^S. Hence, the pairwise exposure intensity μ_{ij}^S is specified as follows:

$$\mu_{ij}^S = \frac{1}{1 + \exp\left(\frac{\kappa\alpha_i^D - \left(X_{ij}'\beta^D + Z_{ij}'\delta^S\right)}{\zeta^S}\right)}.$$

Agency recommendation exposure. This exposure rule functions by repeating a J-period. The spot-exposure sets for doctor i and post j are defined as follows:

$$\begin{cases} \tilde{R}^D_{A,i,t} \equiv \left\{ j \in J \mid \sigma^A_i(t) = j,\ X'_{ij}\beta^P + f'_{ij}\delta^A + \tilde{v}^A_{ijt} > \alpha^P_j + \tilde{v}^A_{ijt0} \right\} \\ \tilde{R}^P_{A,j,t} \equiv \left\{ i \in I \mid \sigma^A_i(t) = j,\ X'_{ij}\beta^P + f'_{ij}\delta^A + \tilde{v}^A_{ijt} > \alpha^P_j + \tilde{v}^A_{ijt0} \right\}, \end{cases}$$

where the difference between δ^P and δ^A, which appears in the preference of post, captures a kind of misperception about the utility achieved by the post—relative to the true deterministic matching utility—when evaluating a match between i and j from the perspective of the mating agents. σ^A_i is a random permutation of $\{1, \ldots, J\}$. Which is drawn independently from σ^S_i. $(\tilde{v}^A_{ijt}, \tilde{v}^A_{ijt0})$ are independent idiosyncratic errors in perceived utility that are not captured by the deterministic components. Their distribution is denoted by H^A. I assume that H^A is a type-I extreme-value distribution with scale parameter ζ^A. Hence, the pairwise exposure intensity μ^A_{ij} is specified as follows:

$$\mu^A_{ij} = \frac{1}{1 + \exp\left(\dfrac{\alpha^P_j - \left(X'_{ij}\beta^P + Z'_{ij}\delta^A \right)}{\zeta^A} \right)}.$$

I denote by $\theta_{\text{expo}} \equiv (\delta^S, \delta^A)$ the tuple of additional parameters governing the misperception terms in the two exposure rules. Let $\Gamma \equiv (\zeta^D, \zeta^P, \zeta^S, \zeta^A)$ collect the scale parameters of all the idiosyncratic error terms. The full parameter vector to be estimated is $\theta \equiv (\theta_{\text{pref}}, \theta_{\text{expo}}, \Gamma, \kappa, \rho)$. When I emphasize the pairwise exposure intensities are dependent on the parameters and the continuation values, I use $\mu^S_{ij}(\theta; \alpha^D_i)$ and $\mu^A_{ij}(\theta; \alpha^P_j)$. For the same purpose, I also use $P^D_{ij}(\theta; \alpha^D_i)$ and $P^P_{ji}(\theta; \alpha^P_j)$.

4.2.2 Likelihood Function

Given the continuation values, α, the likelihood of one data point is constructed as

$$\begin{aligned} L\left(\theta; y_{ij}, \alpha\right) = & \left(P^D_{ij}(\theta; \alpha^D_i)\right)^{a^D_{ij}} \left(1 - P^D_{ij}(\theta; \alpha^D_i)\right)^{1 - a^D_{ij}} \times \left(P^P_{ji}(\theta; \alpha^P_j)\right)^{a^P_{ji}} \left(1 - P^P_{ji}(\theta; \alpha^P_j)\right)^{1 - a^P_{ji}} \\ & \times \left(\mu^S_{ij}(\theta; \alpha^D_i) \left(1 - \frac{J-1}{2J}\, \mu^A_{ij}(\theta; \alpha^P_j) \right) \right)^{\mathbf{1}\left\{ (c^D_{S,i,j}, c^D_{A,i,j}) = (1,0) \right\}} \\ & \times \left(\mu^A_{ij}(\theta; \alpha^P_j) \left(1 - \frac{J+1}{2J}\, \mu^S_{ij}(\theta; \alpha^D_i) \right) \right)^{\mathbf{1}\left\{ (c^D_{S,i,j}, c^D_{A,i,j}) = (0,1) \right\}} \\ & \times \left((1 - \mu^S_{ij}(\theta; \alpha^D_i))(1 - \mu^A_{ij}(\theta; \alpha^P_j)) \right)^{\mathbf{1}\left\{ (c^D_{S,i,j}, c^D_{A,i,j}) = (0,0) \right\}}. \end{aligned}$$

Hence, given α, the log-likelihood function to maximize is defined as $LL(\theta; \alpha) \equiv \sum_{ij} \ln L\left(\theta; y_{ij}, \alpha\right)$.

Lastly, I specify the Bellman equation that determines agents' continuation values when the two exposure rules operate simultaneously. These equations impose nonlinear constraints on α, and I maximize the log-likelihood subject to them. Proposition 4 summarizes the steady system for the Bellman equation. Note that, in comparison to the system (4), the current pairwise exposure intensity, $\hat{\mu}$, depends on the continuation values.

Proposition 4. *Let $\widehat{\mu}_{ij} := \mu^S_{ij} + \mu^A_{ij} - \mu^S_{ij}\mu^A_{ij}$. Under Assumption 2, when the market is sufficiently*

large, the stationary continuation values solve the following system for all i and j,

$$\begin{cases} \alpha_i^D = \frac{\rho}{1-\rho} \sum_{j=1}^{J} \frac{\hat{\mu}_{ij}\left(\theta;\alpha_i^D,\alpha_j^P\right)}{J} P_{ji}^P\left(\theta;\alpha_j^P\right) \zeta^D \ln\left(1+\exp\left(\frac{X_{ij}'\beta^D + Z_{ij}'\delta^D - \kappa\alpha_i^D}{\zeta^D}\right)\right), \\ \alpha_j^P = \frac{\rho\tau}{1-\rho} \sum_{i=1}^{I} \frac{\hat{\mu}_{ij}\left(\theta;\alpha_i^D,\alpha_j^P\right)}{J} P_{ij}^D\left(\theta;\alpha_i^D\right) \zeta^P \ln\left(1+\exp\left(\frac{X_{ij}'\beta^P + Z_{ij}'\delta^P - \alpha_j^P}{\zeta^P}\right)\right). \end{cases} \tag{6}$$

Proof. See Appendix A.6. □

I examine whether the system exhibits a contraction-mapping property analogous to Theorem 1. Appendix A.7 describes sufficient conditions under which the system (6) is a contraction and admits a unique stationary equilibrium. In particular, when J is sufficiently large, these conditions are likely to hold.

4.2.3 Identification and Estimation Procedure

I adopt NFXP algorithm to estimate the model (Rust, 1987). In other words, I repeat (i) solving the fixed point of the system (6) and (ii) update the parameters to maximize the log-likelihood function given the continuation values.

It is widely acknowledged that the discount factor is under-identified in a dynamic model (Magnac and Thesmar, 2002). In this estimation, I fix the discount factor at $\rho = 0.99$. The market has about 2,400 posts per month—roughly 80 per day—and the average shift length is 10 hours (approximately a full day's work). Accordingly, I set $\kappa \approx 1 - \rho^{80} \approx 0.552 \approx 0.55$.

I introduce normalizations to the scale parameters of the distribution of private types: $\zeta^D = 1$ and $\zeta^P = 1$. This is because, for any value of ζ^D and ζ^P, the system (6) and the terms in the system is not altered by scaling the parameters, θ_{pref} and θ_{expo}, and the scale parameters of error terms, ζ^S and ζ^A, with ζ^D and ζ^P. Under the normalizations, all the remaining parameters are identified; in particular, the scale parameters of error terms, ζ^S and ζ^A, are identified as the coefficient attached with the continuation values in μ^S and μ^A. Hence, the parameters to estimate is re-defined as $\theta \equiv \left(\theta_{\text{pref}}, \theta_{\text{expo}}, \zeta^S, \zeta^A\right)$.

4.3 Estimation Results

As a model–fit check, I compare the distributions of the observed numbers of exposures for doctors and posts with the corresponding model–implied expected numbers computed from the estimates. Figure E.4 presents side–by–side histograms: Panel A for doctors and Panel B for posts. The model reproduces the modal mass of the observed distributions well. In terms of means, the doctor–side expectation is 3.142 versus an observed mean of 3.138, and the post–side expectation is 1.454 versus an observed mean of 1.452.

Table 4 reports, for each covariate, the change in that covariate that delivers the same change in the corresponding matching utility as a 10% increase in salary. Because these objects are ratios of coefficients, they are invariant to the scale normalization of the latent errors. Formally, for either the exposure or acceptance stage, and for the doctor or post side, let x denote a covariate and let sal denote log salary. The reported statistic is

$$g_x \;=\; \frac{\beta_{\text{sal}} + \delta_{\text{sal}}}{\beta_x + \delta_x} \cdot \log(1.1) \cdot \frac{\sigma_x}{\sigma_{\text{sal}}},$$

Table 4. Equivalence change in other covariates to a 10% increase in salary

Side	Variable	Equiv. (raw)	SE	z	p	% (distance)	SE % (distance)
Panel A: Self-search Exposure							
Doctor	ln Distance (km)	−0.0553	0.0114	−4.8519	0.0000	−5.3762	1.0777
Doctor	Age	1.1880	0.4185	2.8390	0.0045		
Doctor	Exp (yrs)	2.1914	1.2618	1.7368	0.0824		
Doctor	Hours	−2.1470	0.5345	−4.0168	0.0001		
Panel B: Agency-recommendation Exposure							
Post	ln Distance (km)	0.0773	0.0167	4.6342	0.0000	8.0352	1.8018
Post	Age	1.3317	0.5685	2.3427	0.0191		
Post	Exp (yrs)	−1.7535	0.9632	−1.8206	0.0687		
Post	Hours	−1.0499	0.1591	−6.6004	0.0000		
Panel C: Acceptance (Doctor)							
Doctor	ln Distance (km)	0.0117	0.1274	0.0919	0.9268	1.1776	12.8878
Doctor	Age	0.0083	0.0900	0.0922	0.9266		
Doctor	Exp (yrs)	−0.0117	0.1271	−0.0922	0.9266		
Doctor	Hours	−0.0167	0.1798	−0.0927	0.9262		
Panel D: Acceptance (Post)							
Post	ln Distance (km)	0.9618	0.6803	1.4138	0.1574	161.6455	178.0054
Post	Age	0.7883	0.1218	6.4722	0.0000		
Post	Exp (yrs)	−1.6555	0.3444	−4.8074	0.0000		
Post	Hours	−2.4955	0.4897	−5.0954	0.0000		

Notes: Entries report, for each covariate, the change in raw units that yields the same change in the matching utility term as a 10% increase in salary. SEs use the fixed-α. The percent column is only defined for ln `Distance (km)`.

that is, a ratio of coefficients scaled by the empirical standard deviations $(\sigma_x, \sigma_{\text{sal}})$. Standard errors and p-values are computed from the fixed-α outer likelihood via the observed information and then mapped to g_x using the delta method.[6] For log distance, we also report the implied percentage change to facilitate interpretation on the original scale.

On the exposure margin, both rules continue to show economically meaningful relationships with the covariates. In self-search (Panel A), a 10% salary increase is equivalent to about a 5.38% reduction in distance, indicating doctors' clear preference for nearby posts. Agency recommendation (Panel B) goes the other way: a 10% salary increase corresponds to roughly an 8.04% increase in distance, consistent with the agency casting a geographic distance. Beyond distance, the agency places positive weight on doctor experience—a 10% salary increase trades off against about 1.75 fewer years of experience on the doctor side. By contrast, age is negatively valued on the post side: an increase of about 1.33 years is equivalent to a 10% salary increase in the post's matching utility.

At the acceptance margin, doctor acceptance (Panel C) remains essentially flat with respect to these covariates once exposure has occurred. Post acceptance (Panel D) remains responsive, with the same qualitative signs as in Panel B: a 10% salary increase is comparable to about 0.79 in age, −1.66 years of doctor experience, and −2.50 hours, indicating stronger sorting on the post side at the final decision stage. The distance effect on the post side is large in magnitude (about +161.6%) but imprecise and should therefore be interpreted cautiously; a natural interpretation is that, because the agency and doctors already select nearby matches at the exposure stage, posts care less about a candidate's distance conditional on meeting.

These patterns also hold when I examine the dummy variables that capture whether a doctor's desired job type matches the job description specified by the post side. Table E.1 reports, for these dummies, the same set of estimates and test statistics as Table 4. The doctor-side margin at the acceptance stage is very

[6]The detail of the variance estimation is left to Appendix C. Since the Hessian matrix is so large, I do not compute the Hessian directly. Instead, I adopt a method based on Hessian-vector products and a linear solver.

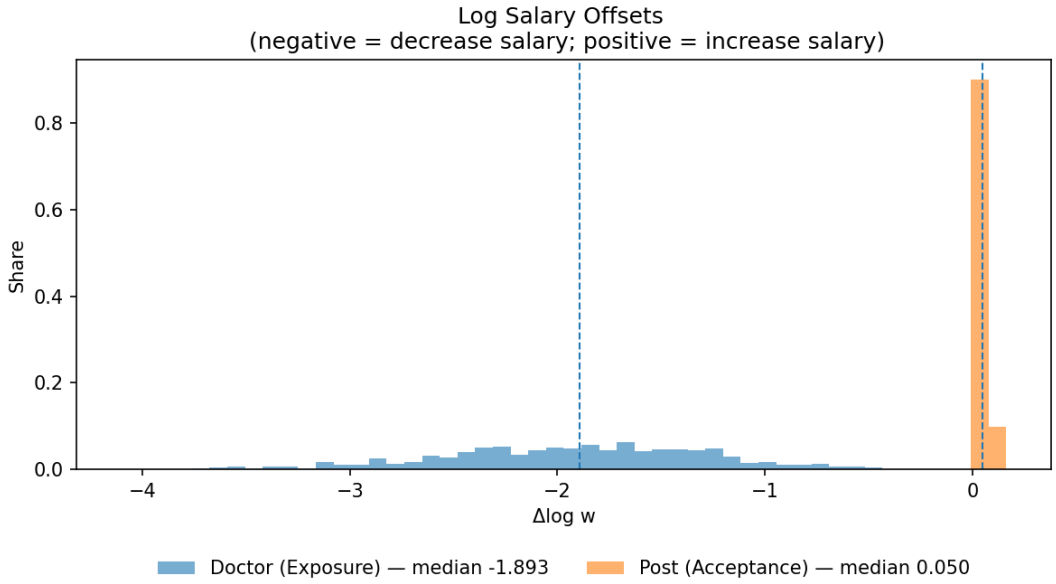

Figure 1. Monetary Measures of Continuation Values

Notes: The figure displays histograms of $\Delta \ln w$ computed from the estimated continuation values and the salary slope s for the selected stage/side. A vertical line marks the median. Negative (positive) bars indicate that a salary cut (raise) in $(e^{|\Delta w|} - 1) \times 100$ percent would leave the probabilities of accept and exposure unchanged if the benefits of remaining, i.e. the continuation values, were removed. See text for the mapping from α to $\Delta \ln w$.

small; most of the doctor-side sorting appears to occur at the self-search exposure stage. By contrast, the post side exhibits relatively strong preferences even at the acceptance stage. This asymmetry is natural: under self-search, the same doctor makes both the exposure and acceptance decisions, while the agency cannot fully internalize or observe the post side's needs, leading to sharper slopes on the post side at acceptance.

Continuation values. I evaluate the continuation values in this platform to reveal which side is *strong* in this market and by how much. For this purpose, I need the "true" preference structure of both sides. Considering the above estimates, it is natural to assume that doctors' preferences are identified from the self-search exposure decisions, whereas post-side preferences are identified from the acceptance decisions. Hence, I use the exposure model estimates (β^D, δ^S) for doctor side and the acceptance model estimates (β^P, δ^P) for post side for below analysis.

I measure continuation values in monetary units using *salary offsets*. Specifically, I compute the change in log salary that equalizes the propensity of self-search exposure or post acceptance between the baseline with the estimated α and the counterfactual with $\alpha = 0$. Let $\beta + \delta$ denote the composite coefficient on $\ln w$. Then

$$\text{Doctor:} \quad -\kappa\,\alpha_i^D + (\beta+\delta)\ln w \;=\; (\beta+\delta)\big(\ln w + \Delta \ln w\big) \;\Rightarrow\; \Delta \ln w \;=\; -\frac{\kappa}{\beta+\delta}\,\alpha_i^D,$$

$$\text{Post:} \quad -\alpha_j^P + (\beta+\delta)\ln w \;=\; (\beta+\delta)\big(\ln w + \Delta \ln w\big) \;\Rightarrow\; \Delta \ln w \;=\; -\frac{1}{\beta+\delta}\,\alpha_j^P.$$

Note that $\beta + \delta > 0$ on the doctor side, whereas $\beta + \delta < 0$ on the post side: doctors prefer higher wages while posts disprefer them. Consequently, the computed salary offsets should be negative for doctors

and positive for posts.

To interpret the salary offsets, it helps to see how continuation values enter decisions. Focus on doctors; the same logic applies to posts. A higher continuation value $\alpha_i^D > 0$ makes a doctor more selective—he is willing to wait longer for better opportunities. If I remove this continuation value by setting $\alpha_i^D = 0$, he searches more aggressively and is exposed to more posts. To keep his exposure propensity at the observed level, the salary must be reduced; the *salary offset* is exactly this required reduction. Specifically, salary must be adjusted by $(e^{\Delta \ln w} - 1) \times 100$ percentage points. Larger absolute offsets correspond to higher continuation values—that is, a platform the doctor finds more valuable.

Figure 1 expresses each side's continuation value in monetary units by plotting the distribution of log salary offsets. The distributions suggest that doctors hold the stronger position in this market: doctor offsets are typically more largely negative (median -1.893, i.e., about an 85% decrease), whereas post offsets are modestly positive (median 0.05, i.e., about a 5% increase), indicating greater selectivity on the doctor side. This pattern is natural given the spot nature of the platform—medical institutions cannot afford to wait. The doctor-side distribution also exhibits greater variance, implying unequal treatment across doctors: more attractive doctors can be highly selective. By contrast, most posts have log salary offsets at or near zero, reflecting that many posts receive few exposures over the sequence.

4.4 Optimal Exposure Rule

This section studies optimal exposure rules by solving instances of **P** (Section 3) under a constraint that fixes each doctor's expected number of exposures at a positive level. As a practical benchmark, I set this target to 40 exposures per doctor per sequence, reflecting Medical Principle's internal guideline that about 40 recommendations per month is optimal: substantially more recommendations tend to overwhelm doctors and make it harder for them to focus on the best opportunities. In particular, when constructing the budget polytope $\mathcal{B}$, I set $c_i^r = l_i^r = 40$ for all i, so that each doctor's expected number of exposures is fixed at 40 per month. I impose no analogous restriction on the post side; that is, c_j^c and l_j^c are not fixed to specific values.

Implementation detail. Algorithm 1 requires solving a linear system to obtain the adjoint vector at each outer step. A naive formulation treats the Jacobian M as a dense $(IJ) \times (IJ)$ matrix, which is prohibitive in both time and memory. To address this, I exploit the block structure of M and apply a *Schur–complement reduction* to a much smaller system. I then solve the reduced linear system with an iterative Krylov method, instead of a direct dense solver. This combination avoids materializing large matrices and enables runs at the platform scale $I = 1{,}132$, $J = 2{,}446$. Details of the techniques used here are provided in Appendix D.

At each outer step of Algorithm 1, I solve the fixed point $G(\alpha, \mu) = 0$, form $K = q \odot \exp(\nabla U/\varepsilon)$, and project K onto the budget set. In the application here the feasible set imposes only *row equalities* and box constraints: $\sum_j \mu_{ij} = 40$ for all i and $0 \le \mu_{ij} \le 1$, with no binding column constraints. Hence the projector reduces to two updates per cycle: a row-equality scaling and a box clip, which makes the computation light. The baseline exposure intensity q is a row-normalized temperature softmax of $U^{\det} + V^{\det\top}$. I start from a fixed temperature $\varepsilon = 0.03$, and use damping $\theta = 0.3$, and: (i) value fixed point: (max iters $= 300$, tol $= 10^{-8}$, damp $= 0.5$); (ii) Bregman–Dykstra projector: (max iters $=$

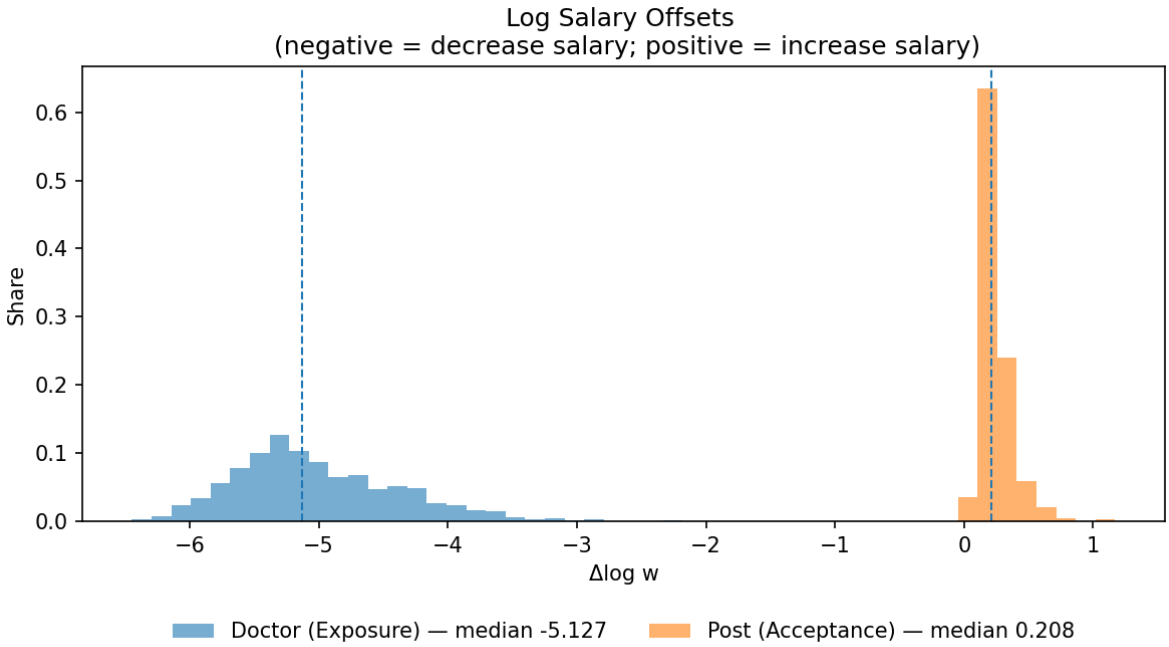

Figure 2. Monetary Measures of Continuation Values under Optimal Bernoulli Exposure Rule

Notes: The figure displays histograms of $\Delta \ln w$ computed from the computed continuation values and the estimated salary slope s for the selected stage/side. A vertical line marks the median. Negative (positive) bars indicate that a salary cut (raise) in $(e^{|\Delta w|} - 1) \times 100$ percent would leave the probabilities of accept and exposure unchanged if the benefits of remaining, i.e. the continuation values, were removed. See text for the mapping from α to $\Delta \ln w$.

800, $\text{tol} = 10^{-6}$, $\eta = 0.5$).

Optimal exposure. Figure 2 reports log salary offsets of continuation values under the optimal exposure rule. The distributions again indicate that doctors hold the stronger position: doctor offsets are typically more negative (median -5.127, i.e., about a 99% decrease), whereas post offsets are modestly positive (median 0.208, i.e., about a 23% increase), consistent with greater selectivity on the doctor side. Relative to the realized market in Figure 1, both sides become more selective under the current rule—the medians move farther from zero in magnitude. Moreover, the variance on the post side rises substantially (from 0.02 on the actual platform to 0.13 under the optimal rule), reflecting a wider dispersion: many posts are exposed to more doctors under this exposure rule and at the same time the inequality among posts grows.

In Table E.2, I regress log salary offsets on post- and doctor-side covariates, using $\Delta \ln w$ for posts and $-\Delta \ln w$ for doctors so that positive coefficients indicate larger absolute offsets. On the post side, the on-call indicator is the dominant correlate, with a large positive association, while longer scheduled hours are negatively related. Among content features, many covariates load negatively on the offset, with the house-call indicator an exception that loads positively. On the doctor side, demographic variables contribute little on average, whereas practice-content indicators are more informative: preferences aligned with outpatient care, inpatient ward care, and endoscopy are the top three associated with larger absolute offsets. Overall, value concentrates on specific post attributes (especially on-call duties) and on doctors whose revealed content preferences align with those high-value posts.

Table 5. How the exposure design changes doctor–post attribute relations

Panel A: Doctor/Post-only attributes		$\hat{b}$	$b^\star$	$\Delta = b^\star - \hat{b}$	SE(Δ)	z	p
Hours	Age	−0.011	0.008	0.019	0.008	2.308	0.021
Hours	Experience	−0.002	−0.002	0.000	0.008	0.056	0.956
Log salary	Age	0.000	−0.001	−0.001	0.000	−1.735	0.083
Log salary	Experience	−0.001	0.001	0.001	0.000	3.340	0.001
Panel B: Distance effects							
Distance (bps per +10%)		−3.612	0.163	3.776	0.001	3544.882	0.000

Notes: Panel A reports OLS coefficients linking (doctor attributes) to (post-side attribute weighted averages) under the baseline exposure $\hat{\iota}$ and the optimized exposure $\iota^\star$, with $\Delta = b^\star - \hat{b}$ and a Wald test for $H_0 : \Delta = 0$. Panel B reports semi-elasticities of exposure with respect to distance in two units: basis points (bps) per +10% increase in distance.

Comparison with actual exposure rule. To compare the baseline exposure $\hat{\mu}$ with the optimal exposure $\mu^\star$, I run two complementary regressions. First, for each doctor i, I form the μ–weighted average of a post attribute x_j^P, $\bar{x}_i^P(\mu) = \sum_j \mu_{ij} x_j^P$, and regress it on doctor covariates x_i^D in pooled OLS across doctors: $\bar{x}_i^P(\mu) = \beta_0(\mu) + x_i^{D\top}\beta(\mu) + \varepsilon_i$. I estimate this twice—once with $\mu = \hat{\mu}$ and once with $\mu = \mu^\star$—and report $\hat{b}$, $b^\star$, and their difference $\Delta = b^\star - \hat{b}$ with a Wald test for $H_0 : \Delta = 0$. Second, because distance is pair specific, I regress μ_{ij} on $\ln(\text{distance}_{ij})$ at the pair level. I report *basis points per* +10% *increase in distance*, computed as $c \times \ln(1.1) \times 10{,}000$, where c is the log-distance coefficient. For each exposure rule ($\hat{\mu}$ and $\mu^\star$) I report the slope and, using a standard Wald test, the difference between the two slopes with its standard error and p-value.

Table 5 summarizes the comparisons. Panel A is about the side-specific attributes and Panel B is about the pair-specific attribute. Two shifts in Panel A are noteworthy. First, the Hours–Age slope flips sign: under the baseline, older doctors are weakly tilted toward posts with fewer hours, whereas under the optimized rule they are tilted toward posts with more hours. Second, the Log-salary–Age slope becomes more negative, indicating a mild reweighting away from the very highest-salary posts for older doctors. The Log-salary–Experience slope turns positive, pointing to more experienced doctors being steered toward higher-wage posts under the optimized exposure. Panel B shows a change in the distance semi-elasticity. In the baseline, exposure falls with distance: about −3.61 bps per +10% distance. Under the optimized rule the slope is essentially flat to slightly positive: about +0.16 bps per +10%. In other words, the optimal design largely removes the baseline penalty on distance, making exposure far more distance-neutral.

Source of user value. I investigate the sources of user value generated under the optimal exposure. To that end, I compute an alternative rule that fixes each doctor's expected number of exposures at its estimated level. Specifically, using the estimates, I obtain $\hat{\mu}_{ij}$ for all doctor–post pairs and define, for each doctor i, the estimated expected number of exposures in a sequence as $\xi_i \equiv \sum_j \hat{\mu}_{ij}$. I then set the budget polytope to

$$\hat{\mathcal{B}} = \Big\{\mu \in [0,1]^{I\times J} : \sum_j \mu_{ij} = \xi_i \ \ \forall i\Big\},$$

and solve the resulting optimal exposure problem **P**.

The distribution of log salary offsets under this rule is shown in Figure 3. The medians on both sides are smaller in magnitude than in the realized market (Figure 1): on the doctor side, the median implies only a 26% salary reduction (85% in the actual market), and on the post side, the median implies about a 1% salary increase (5% in the actual marker). This pattern indicates that the primary source of user-

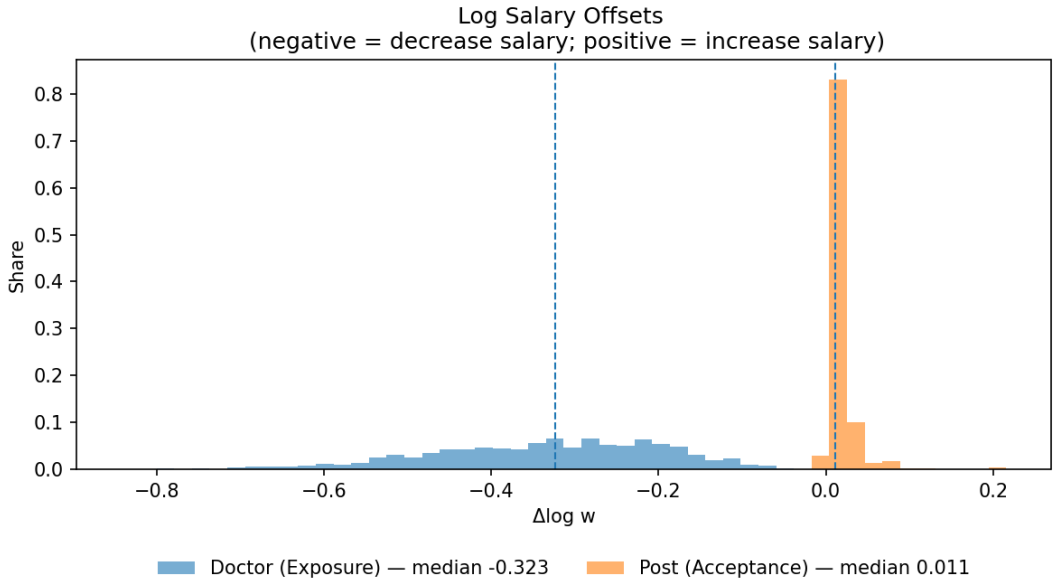

Figure 3. Monetary Measures of Continuation Values under Optimal Exposure Rule with Same # Exposures

Notes: The figure displays histograms of $\Delta \ln w$ computed from the computed continuation values and the estimated salary slope s for the selected stage/side. A vertical line marks the median. Negative (positive) bars indicate that a salary cut (raise) in $(e^{|\Delta w|} - 1) \times 100$ percent would leave the probabilities of accept and exposure unchanged if the benefits of remaining, i.e. the continuation values, were removed. See text for the mapping from α to $\Delta \ln w$.

value gains under the optimal Bernoulli design with 40 exposures per doctor is the *scale* of exposures. In simulations, the median log salary offsets on both sides remain below their realized-market levels unless I raise each doctor's expected exposures to about seven times the realized level—that is, set ξ_i to 7× its empirical value.

The simulations indicate that the realized market achieves relatively high user value: holding the expected exposures per doctor fixed, the optimal Bernoulli design does not exceed the realized market's user value, as evidenced by the smaller median log salary offsets under the optimal rule. This remains true even though the optimal Bernoulli rule maximizes user value within its budget polytope. The mechanism behind this finding is that the realized platform's exposure rule is *endogenous* to continuation values—the Bellman system governing the realized market differs from that in the exogenous optimal-design problem. Under both self-search and agency-recommendation exposure rules, targets are selected precisely when the match utility exceeds the relevant continuation value, thereby creating a selection that raises user value relative to a design that sets exposure rules without conditioning on those continuation values. In other words, a preference-aware exposure rule exploits users' tastes and thus boosts user value, but it cannot directly control the number of exposures; the optimal-design rule, by contrast, can finely control exposure counts but less exploit users' preference. Platforms must balance these trade-offs to tailor an exposure rule suited to the market they face.

5 Conclusion

This paper studied how exposure design on two-sided search platforms can create a wedge between maximizing flow match surplus today and maximizing long-run user value. I formalized this wedge by explicitly modeling participants' continuation values as the fixed point of a dynamic system, showing how exposure rules that pull forward high-surplus pairs also lowers the value of options left for the remaining participants and depress future acceptance prospects. Building on this insight, I posed the platform's problem of user–value maximization and developed a tractable computational approach that combines entropic regularization, an adjoint-based gradient, and a fixed point problem. The method selects among multiple optima in a principled way and is practical at marketplace scale.

Applying the framework to a doctor–spot-job platform, I estimated preferences and exposure rules implemented there, recovered continuation values, and computed the user–value–maximizing exposure rule. Relative to the implemented rule, the optimal exposure rule raises both sides' continuation values in salary-offset terms. Attribute regressions indicate that on-call posts and doctors with certain service preferences gain most, while demographics matter little. Together, these results demonstrate that exposure policies tuned to long-run user value can differ meaningfully from the actually implemented rules.

Discussion. In the empirical specification, acceptance decisions do not admit additional unobserved selection induced by the exposure stage: i.e., no latent shock carried from exposure into acceptance beyond observed covariates. This exclusion greatly simplifies the likelihood—exposure can be treated as predetermined when forming the acceptance component—yet it is plausibly too strong. A richer model could (i) introduce pair- or side-specific random effects shared across exposure and acceptance, (ii) use a control–function or copula link between the two stages, or (iii) leverage timing and quasi-random variation in exposure intensity to identify selection at acceptance. Each approach preserves the fixed-point structure for continuation values but requires either simulation-based likelihood or composite likelihood to remain tractable.

Our analysis targets a stationary environment. Practical recommendations, however, operate under nonstationary demand, seasonality, and policy drift. Then, extending the algorithm proposed here to an online algorithm is a promising direction: maintain running estimates of continuation values; update the adjoint; and perform one or a few Sinkhorn steps per batch of new data. Such an online version of the algorithm could optimize a long-run user value while tracking shifts in primitives. Formal guarantees and engineering choices are key open tasks.

References

Adachi, Hiroyuki. 2003. "A search model of two-sided matching under nontransferable utility." *Journal of Economic Theory*, 113(2): 182–198.

Benamou, Jean-David, Guillaume Carlier, Marco Cuturi, Luca Nenna, and Gabriel Peyré. 2014. "Iterative Bregman Projections for Regularized Transportation Problems."

Biega, Asia J., Krishna P. Gummadi, and Gerhard Weikum. 2018. "Equity of Attention: Amortizing Individual Fairness in Rankings." *SIGIR '18*, 405–414. ACM.

Chen, Kuan-Ming, Yu-Wei Hsieh, and Ming-Jen Lin. 2023. "REDUCING RECOMMENDATION INEQUALITY VIA TWO-SIDED MATCHING: A FIELD EXPERIMENT OF ONLINE DATING." *International Economic Review*, 64(3): 1201–1221.

Cuturi, Marco. 2013. "Sinkhorn distances: lightspeed computation of optimal transport." *NIPS'13*, 2292–2300. Red Hook, NY, USA:Curran Associates Inc.

Dudík, Miroslav, John Langford, and Lihong Li. 2011. "Doubly robust policy evaluation and learning." *ICML'11*, 1097–1104. Madison, WI, USA:Omnipress.

Gale, D., and L. S. Shapley. 1962. "College Admissions and the Stability of Marriage." *The American Mathematical Monthly*, 69(1): 9–15.

Grover, Aditya, Eric Wang, Aaron Zweig, and Stefano Ermon. 2019. "Stochastic Optimization of Sorting Networks via Continuous Relaxations." International Conference on Learning Representations. ICLR.

Hitsch, Gunter J., Ali Hortaçsu, and Dan Ariely. 2010. "Matching and Sorting in Online Dating." *American Economic Review*, 100(1): 130–163.

Ie, Eugene, Vihan Jain, Jing Wang, Sanmit Narvekar, Ritesh Agarwal, Rui Wu, Heng-Tze Cheng, Tushar Chandra, and Craig Boutilier. 2019. "SLATEQ: a tractable decomposition for reinforcement learning with recommendation sets." *IJCAI'19*, 2592–2599. AAAI Press.

Jambor, Tamas, and Jun Wang. 2010. "Optimizing multiple objectives in collaborative filtering." *RecSys '10*, 55–62. Association for Computing Machinery.

Magnac, Thierry, and David Thesmar. 2002. "Identifying Dynamic Discrete Decision Processes." *Econometrica*, 70(2): 801–816.

Mena, Gonzalo, David Belanger, Scott Linderman, and Jasper Snoek. 2018. "Learning Latent Permutations with Gumbel-Sinkhorn Networks." International Conference on Learning Representations. ICLR.

Prillo, Sebastian, and Julian Martin Eisenschlos. 2020. "SoftSort: a continuous relaxation for the argsort operator." *ICML'20*. JMLR.org.

Rust, John. 1987. "Optimal Replacement of GMC Bus Engines: An Empirical Model of Harold Zurcher." *Econometrica*, 55(5): 999–1033.

Shapley, Lloyd S, and Martin Shubik. 1971. "The assignment game I: The core." *International Journal of game theory*, 1(1): 111–130.

Shi, Peng. 2023. "Optimal Matchmaking Strategy in Two-Sided Marketplaces." *Management Science*, 69(3): 1323–1340.

Shi, Peng. 2025. "Optimal Match Recommendations in Two-sided Marketplaces with Endogenous Prices." *Management Science*, 71(9): 7431–7448.

Sürer, Özge, Robin Burke, and Edward C. Malthouse. 2018. "Multistakeholder recommendation with provider constraints." *RecSys '18*, 54–62. Association for Computing Machinery.

Swaminathan, Adith, and Thorsten Joachims. 2015. "Counterfactual Risk Minimization." *WWW '15 Companion*, 939–941. New York, NY, USA:Association for Computing Machinery.

Wang, Yuyan, Long Tao, and Xian Xing Zhang. 2025. "Recommending for a Multi-Sided Marketplace: A Multi-Objective Hierarchical Approach." *Marketing Science*, 44(1): 1–29.

A Omitted proofs

A.1 When does prob of no overlap go to 0?

Let

$$P_{I,J} \;=\; \Pr(\text{no overlap}) \;=\; \prod_{k=0}^{I-1}\Big(1-\frac{k}{J}\Big), \qquad 1 \le I \le J,$$

denote the probability that I agents, each independently selecting one of J goods, make distinct choices.

General expansion (valid for all $I \le J$). Using $\log(1-y) = -y - \frac{y^2}{2} - \frac{y^3}{3} - \dots$ $(0 < y < 1)$,

$$\log P_{I,J} = -\frac{I(I-1)}{2J} - \frac{(I-1)I(2I-1)}{12J^2} + R_{I,J}, \qquad |R_{I,J}| \;<\; \frac{I^4}{12J^3}. \tag{7}$$

Square–root barrier. Set $I = I(J)$ and let $J \to \infty$.

(i) **Sub-critical regime.** If $I = o(\sqrt{J})$ (equivalently $I^2/J \to 0$), every term in (7) vanishes, hence

$$P_{I,J} = 1 - o(1).$$

The no–overlap event occurs with probability tending to 1.

(ii) **Critical window.** If $I \sim c\sqrt{J}$ with constant $c > 0$, then

$$\log P_{I,J} \;\longrightarrow\; -\frac{c^2}{2}, \qquad P_{I,J} \;\longrightarrow\; e^{-c^2/2} \in (0,1).$$

The probability converges to a non–degenerate limit.

(iii) **Super-critical regime.** If $\sqrt{J} \ll I \le o(J)$, the leading term $-\frac{I^2}{2J} \to -\infty$, so

$$P_{I,J} \;\longrightarrow\; 0,$$

making collisions virtually certain. (When I is a fixed fraction of J, the same exponential decay was obtained earlier.)

Summary. The necessary and sufficient condition for

$$\Pr(\text{no overlap}) \;\xrightarrow[J\to\infty]{}\; 1$$

is

$$I = o\big(\sqrt{J}\big) \;\iff\; \frac{I^2}{J} \;\xrightarrow[J\to\infty]{}\; 0.$$

The scale $I \asymp \sqrt{J}$ constitutes a sharp *square-root threshold* separating regimes of almost-sure uniqueness from almost-sure collisions.

A.2 Proof of Theorem 1

Lemma 1 (Lipschitz bound (Bernoulli exposure)). *Let $g = (g^D, g^P)$ be the time–homogeneous map induced by the stationary version of* (4) *under the Bernoulli exposure rule: each doctor i draws a per-*

mutation σ_i of J posts at the beginning of each sequence, and in period t an exposure between i and $j = \sigma_i(t)$ occurs with probability μ_{ij}, independently across i and t conditional on $(\sigma_i)_i$. Let W^D, W^P be defined by (2)–(3).

Assume:

1. *Deterministic parts are bounded: $|\tilde{U}_{ij}^{\det}| \le \overline{\tilde{U}}$, $|V_{ji}^{\det}| \le \bar{V}$, and $\mathbb{E}[|\varepsilon^D|], \mathbb{E}[|\varepsilon^P|] < \infty$.*

2. *Type shocks are independent and admit bounded densities: $\varepsilon^D \perp\!\!\!\perp \varepsilon^P$, $\sup_x f_D(x) \le \bar{f}_D$, $\sup_y f_P(y) \le \bar{f}_P$.*

3. *Define the* exposure-mass *bounds*

$$\gamma_{\max}^D := \max_i \frac{1}{J} \sum_{j \in J} \mu_{ij}, \qquad \gamma_{\max}^P := \max_j \tau \, \frac{1}{J} \sum_{i \in I} \mu_{ij}, \qquad \text{where } \tau := \left(\tfrac{J-1}{J}\right)^{I-1}.$$

Set

$$C_D^{(\kappa)} := \overline{\tilde{U}} + \mathbb{E}[|\varepsilon^D|], \qquad C_P := \bar{V} + \mathbb{E}[|\varepsilon^P|], \qquad C_*^{(\kappa)} := \max\{\gamma_{\max}^D C_D^{(\kappa)},\ \gamma_{\max}^P C_P\}.$$

Fix $R \ge \dfrac{\rho}{1-\rho}\, C_*^{(\kappa)}$ and write $B_R := \{\alpha : \|\alpha\|_\infty \le R\}$.

Then $g(B_R) \subseteq B_R$ and, for all $\alpha, \alpha' \in B_R$,

$$\|g(\alpha) - g(\alpha')\|_\infty \ \le \ q_R^{(\kappa)} \, \|\alpha - \alpha'\|_\infty,$$

with

$$q_R^{(\kappa)} := \rho \ \max\Big\{ \ \gamma_{\max}^D \big[1 + \bar{f}_P \, (R + C_D^{(\kappa)})\big],\ \gamma_{\max}^P \big[1 + \kappa \, \bar{f}_D \, (R + C_P)\big] \Big\}.$$

In particular, if $q_R^{(\kappa)} < 1$, the stationary system $\alpha = g(\alpha)$ admits a unique fixed point in B_R.

Proof. Throughout write $a = \alpha_i^D$, $b = \alpha_j^P$, $a' = \alpha_i^{D\prime}$, $b' = \alpha_j^{P\prime}$, and note $|a|, |a'|, |b|, |b'| \le R$ on B_R.

Prelim: Bernoulli exposure implies weights μ_{ij}/J. Under the Bernoulli exposure rule,

$$\Pr\big(j \in \tilde{R}_{i,t}^D\big) = \Pr(\sigma_i(t) = j) \Pr(X_{i,t} = 1 \mid \sigma_i(t) = j) = \frac{1}{J} \mu_{ij},$$

where $X_{i,t} \sim \text{Bernoulli}(\mu_{i,\sigma_i(t)})$. Under Assumption 2 (large market), the post-side overlap adjustment yields $\Pr(i \in \tilde{R}_{j,t}^P) \approx \tau \, \mu_{ij}/J$ with $\tau = ((J-1)/J)^{I-1}$. Therefore, suppressing t, the stationary form of (4) can be written as

$$\alpha_i^D \ = \ \rho \, \alpha_i^D \ + \ \rho \sum_j \frac{\mu_{ij}}{J} \underbrace{\mathbb{E}\big[\mathbf{1}\{V_{ji}^{\det} + \varepsilon^P > b\} \, \max\{\tilde{U}_{ij}^{\det} - \kappa a + \varepsilon^D, 0\}\big]}_{=: \, \widetilde{W}^D(a,b)},$$

$$\alpha_j^P \ = \ \rho \, \alpha_j^P \ + \ \rho \, \tau \sum_i \frac{\mu_{ij}}{J} \underbrace{\mathbb{E}\big[\mathbf{1}\{\tilde{U}_{ij}^{\det} + \varepsilon^D > \kappa a\} \, \max\{V_{ji}^{\det} - b + \varepsilon^P, 0\}\big]}_{=: \, \widetilde{W}^P(a,b)}.$$

Equivalently, $(1-\rho)\alpha = \widetilde{g}(\alpha)$ where $\widetilde{g}_i^D(\alpha) := \rho \sum_j \frac{\mu_{ij}}{J} \widetilde{W}^D(a,b)$ and $\widetilde{g}_j^P(\alpha) := \rho \, \tau \sum_i \frac{\mu_{ij}}{J} \widetilde{W}^P(a,b)$. The Lipschitz properties of g and $\widetilde{g}$ coincide, so it is enough to work with $\widetilde{W}$.

Step 1: Lipschitz bounds for $\widetilde{W}^D, \widetilde{W}^P$. By independence,

$$\widetilde{W}^D(a,b) = \mathbb{E}[\max\{\tilde{U}^{\det} - \kappa a + \varepsilon^D, 0\}] \cdot \Pr(V^{\det} + \varepsilon^P > b),$$

$$\widetilde{W}^P(a,b) = \Pr(\tilde{U}^{\det} + \varepsilon^D > \kappa a) \cdot \mathbb{E}[\max\{V^{\det} - b + \varepsilon^P, 0\}].$$

(own–argument). The maps $a \mapsto \max\{\tilde{U}^{\det} - \kappa a + \varepsilon^D, 0\}$ and $b \mapsto \max\{V^{\det} - b + \varepsilon^P, 0\}$ are κ– and 1–Lipschitz, respectively. Multiplying by probabilities in $[0,1]$ preserves Lipschitz moduli, hence

$$|\widetilde{W}^D(a,b) - \widetilde{W}^D(a',b)| \le |a - a'|, \qquad |\widetilde{W}^P(a,b) - \widetilde{W}^P(a,b')| \le |b - b'|.$$

(cross–argument). Let F_P be the CDF of $V^{\det} + \varepsilon^P$ and F_D that of $\tilde{U}^{\det} + \varepsilon^D$. Since F_P, F_D are $\bar{f}_P, \bar{f}_D$–Lipschitz,

$$|\Pr(V^{\det} + \varepsilon^P > b) - \Pr(V^{\det} + \varepsilon^P > b')| \le \bar{f}_P\,|b - b'|,$$

$$|\Pr(\tilde{U}^{\det} + \varepsilon^D > \kappa a) - \Pr(\tilde{U}^{\det} + \varepsilon^D > \kappa a')| \le \kappa\,\bar{f}_D\,|a - a'|.$$

Moreover, for $|a|, |b| \le R$,

$$\mathbb{E}[\max\{\tilde{U}^{\det} - \kappa a + \varepsilon^D, 0\}] \le \mathbb{E}[|\tilde{U}^{\det} + \varepsilon^D|] + \kappa|a| \le C_D^{(\kappa)} + R \le R + C_D^{(\kappa)},$$

$$\mathbb{E}[\max\{V^{\det} - b + \varepsilon^P, 0\}] \le \mathbb{E}[|V^{\det} + \varepsilon^P|] + |b| \le C_P + R \le R + C_P.$$

Therefore

$$|\widetilde{W}^D(a,b) - \widetilde{W}^D(a,b')| \le (R + C_D^{(\kappa)})\,\bar{f}_P\,|b - b'|, \quad |\widetilde{W}^P(a,b) - \widetilde{W}^P(a',b)| \le \kappa\,(R + C_P)\,\bar{f}_D\,|a - a'|.$$

Step 2: Lipschitz bound for g. Using Step 1,

$$\begin{aligned} |g_i^D(\alpha) - g_i^D(\alpha')| &\le \rho \sum_j \frac{\mu_{ij}}{J} \Big(|\alpha_i^D - \alpha_i^{D\prime}| + \bar{f}_P(R + C_D^{(\kappa)})\,\|\alpha^P - \alpha^{P\prime}\|_\infty \Big) \\ &\le \rho \Big(\sum_j \frac{\mu_{ij}}{J} \Big) \big[\, 1 + \bar{f}_P(R + C_D^{(\kappa)}) \,\big]\ \|\alpha - \alpha'\|_\infty. \end{aligned}$$

Taking sup over i yields

$$\|g^D(\alpha) - g^D(\alpha')\|_\infty \le \rho\,\gamma_{\max}^D \big[1 + \bar{f}_P(R + C_D^{(\kappa)})\big]\ \|\alpha - \alpha'\|_\infty.$$

Similarly,

$$\|g^P(\alpha) - g^P(\alpha')\|_\infty \le \rho\,\gamma_{\max}^P \big[1 + \kappa\,\bar{f}_D(R + C_P)\big]\ \|\alpha - \alpha'\|_\infty.$$

Combining gives the stated $q_R^{(\kappa)}$.

Step 3: $g(B_R) \subseteq B_R$. From the rearranged form (Prelim),

$$|g_i^D(\alpha)| \le \rho \sum_j \frac{\mu_{ij}}{J}\,\mathbb{E}[\max\{\tilde{U}^{\det} - \kappa a + \varepsilon^D, 0\}] \le \rho \Big(\sum_j \frac{\mu_{ij}}{J} \Big)\,(R + C_D^{(\kappa)}),$$

$$|g_j^P(\alpha)| \le \rho\,\tau \sum_i \frac{\mu_{ij}}{J}\,\mathbb{E}[\max\{V^{\det} - b + \varepsilon^P, 0\}] \le \rho\Big(\tau \sum_i \frac{\mu_{ij}}{J}\Big)\,(R + C_P).$$

Hence

$$\|g(\alpha)\|_\infty \le \rho \max\big\{\gamma_{\max}^D(R + C_D^{(\kappa)}),\ \gamma_{\max}^P(R + C_P)\big\} \le \rho\,(R + C_*^{(\kappa)}).$$

By the choice $R \ge \frac{\rho}{1-\rho}\,C_*^{(\kappa)}$ we have $\rho(R + C_*^{(\kappa)}) \le R$, thus $g(B_R) \subseteq B_R$. □

A.3 Proof of Proposition 2

Step 0: Adjoint representation of $\nabla_\mu U(\mu)$. Let $\widehat{U}(\mu) := \sum_i \alpha_i^D(\mu) + \sum_j \alpha_j^P(\mu)$ so that $U(\mu) = \widehat{U}(\mu)/\rho$. By the implicit function theorem applied to $G(\alpha, \mu) = 0$,

$$M\,\frac{\partial \alpha}{\partial \mu_{ij}} + \frac{\partial G}{\partial \mu_{ij}} = 0, \qquad M := \frac{\partial G}{\partial \alpha}(\alpha, \mu).$$

Hence $\frac{\partial \alpha}{\partial \mu_{ij}} = -M^{-1}\frac{\partial G}{\partial \mu_{ij}}$ and

$$\frac{\partial \widehat{U}}{\partial \mu_{ij}} = \nabla_\alpha \widehat{U}^\top \frac{\partial \alpha}{\partial \mu_{ij}} = -\,\nabla_\alpha \widehat{U}^\top M^{-1}\frac{\partial G}{\partial \mu_{ij}}.$$

Define the adjoint vector $\pi = (\pi^D, \pi^P)$ by

$$M^\top \pi = \nabla_\alpha \widehat{U} = (\mathbf{1}_I, \mathbf{1}_J)^\top,$$

to obtain

$$\frac{\partial \widehat{U}}{\partial \mu_{ij}} = -\,\pi^\top \frac{\partial G}{\partial \mu_{ij}}.$$

Step 1: Computing $\partial G/\partial \mu_{ij}$ (holding α fixed). Since $G = \alpha - g$, we have $\partial G/\partial \mu_{ij} = -\,\partial g/\partial \mu_{ij}$. Under the Bernoulli exposure rule (Definition 1), the stationary mapping g has the form

$$g_i^D(\alpha, \mu) = \rho\,\alpha_i^D + \frac{\rho}{J}\sum_{j'} \mu_{ij'}\big(W_{ij'}^D - \alpha_i^D\big), \qquad g_j^P(\alpha, \mu) = \rho\,\alpha_j^P + \frac{\rho\,\tau}{J}\sum_{i'} \mu_{i'j}\big(W_{i'j}^P - \alpha_j^P\big),$$

so that

$$\frac{\partial g_i^D}{\partial \mu_{ij}} = \frac{\rho}{J}\big(W_{ij}^D - \alpha_i^D\big), \qquad \frac{\partial g_j^P}{\partial \mu_{ij}} = \frac{\rho\,\tau}{J}\big(W_{ij}^P - \alpha_j^P\big),$$

and all other components are zero. Therefore,

$$\frac{\partial \widehat{U}}{\partial \mu_{ij}} = \pi^\top \frac{\partial g}{\partial \mu_{ij}} = \frac{\rho}{J}\Big[\ \pi_i^D\big(W_{ij}^D - \alpha_i^D\big) + \tau\,\pi_j^P\big(W_{ij}^P - \alpha_j^P\big)\ \Big].$$

Dividing by ρ yields

$$\nabla_\mu U(\mu)_{ij} = \frac{1}{J}\Big[\ \pi_i^D\big(W_{ij}^D - \alpha_i^D\big) + \tau\,\pi_j^P\big(W_{ij}^P - \alpha_j^P\big)\ \Big]. \tag{8}$$

Step 2: Wedge with the flow objective and the nonnegativity at $\mu_{\text{flow}}^\star$. For an interior maximizer $\mu_{\text{flow}}^\star$ of $S(\mu)$ we have $\nabla_\mu S(\mu_{\text{flow}}^\star) = 0$. Substituting this first-order condition into (8) and rearranging gives

$$\nabla_\mu U(\mu_{\text{flow}}^\star)_{ij} = \frac{1}{J}\Big[\ \pi_i^D(\mu_{\text{flow}}^\star)\big(W_{ij}^D - \alpha_i^D\big) + \tau\,\pi_j^P(\mu_{\text{flow}}^\star)\big(W_{ij}^P - \alpha_j^P\big)\ \Big].$$

If $\pi(\mu^\star_{\text{flow}}) \geq 0$ componentwise, then the bracketed term is weakly nonnegative for all (i,j), hence $\nabla_\mu U(\mu^\star_{\text{flow}})_{ij} \geq 0$ for all (i,j), which proves Proposition 2. □

A.4 Sufficient condition for non-negative adjoint vector

Proposition 5 (EV1 case)**.** *Assume Lemma 1's conditions, and in addition: $\varepsilon^D, \varepsilon^P$ are independent Type I extreme value (unit scale); $\tilde{U}^{\text{det}}_{ij}, V^{\text{det}}_{ji} \in [0,1]$; $\mu \in \mathcal{B}$ with row/column budgets. Let*

$$C_0 := 1 + \sqrt{\tfrac{\pi^2}{6} + \gamma^2} \quad (\gamma: \textit{ Euler's constant}), \qquad R := \frac{\rho}{1-\rho}\,\frac{C_0}{J}, \qquad \tau := \Big(\tfrac{J-1}{J}\Big)^{I-1}.$$

Let $M := \partial_\alpha G(\alpha, \mu)$ at the fixed point and define $\pi = (\pi^D, \pi^P)$ by $M^\top \pi = (\mathbf{1}_I, \mathbf{1}_J)^\top$. If

$$1-\rho \;>\; \frac{\rho}{J\,e}\,\kappa\,(R + C_0) \quad \textit{and} \quad 1-\rho \;>\; \frac{\rho}{J\,e}\,\tau\,(R + C_0), \tag{9}$$

then $\pi \geq 0$ componentwise. A single sufficient condition is

$$1-\rho \;>\; \frac{\rho\, C_0}{e\, J}\,\max\{\kappa, \tau\}\Big(1 + \frac{\rho}{(1-\rho)\,J}\Big), \tag{10}$$

and a coarse, easy-to-check form is

$$J \;>\; \frac{\rho\, C_0}{e\,(1-\rho)}\,\max\{\kappa, \tau\}. \tag{11}$$

Proof. Write the adjoint system as the Z–matrix linear system $L\binom{\pi^D}{\pi^P} = \binom{\mathbf{1}_I}{\mathbf{1}_J}$ with $L = \begin{bmatrix} (1-a) & -B^\top \\ -D & (1-c) \end{bmatrix}$, where $(1-a) := \text{diag}(1 - \partial g^D_i/\partial a_i)$, $(1-c) := \text{diag}(1 - \partial g^P_j/\partial b_j)$, $B_{ji} := -\partial g^P_j/\partial a_i \geq 0$, $D_{ij} := -\partial g^D_i/\partial b_j \geq 0$. Row–wise strict diagonal dominance implies L is a nonsingular M–matrix, hence $L^{-1} \geq 0$ and $\pi = L^{-1}\mathbf{1} \geq 0$. Under EV1 and bounded supports, the cross sums satisfy $\sum_j B_{ji} \leq \frac{\rho}{J\,e}\,\kappa\,(R + C_0)$ and $\sum_i D_{ij} \leq \frac{\rho}{J\,e}\,\tau\,(R + C_0)$, while $1 - a_i, 1 - c_j \geq 1 - \rho$; this yields (9), and the relaxations (10)–(11) follow by upper-bounding. □

A.5 Proof of Proposition 3

Proof. Take $(c^D_{S,i,j}, c^D_{A,i,j}) = (1,0)$ as an example. The probability of this case is computed as follows:

$$
\begin{aligned}
&\Pr\big((c^D_{S,i,j}, c^D_{A,i,j}) = (1,0)\big) \\
&= \sum_{t_1=1}^{J}\sum_{t_2=1}^{J} \Pr\left(\sigma_i^S(t_1) = j, \sigma_i^A(t_2) = j\right) \times \Pr\left((c^D_{S,i,j}, c^D_{A,i,j}) = (1,0) \mid \sigma_i^S(t_1) = j, \sigma_i^A(t_2) = j\right) \\
&= \sum_{t_1=1}^{J}\sum_{t_2=1}^{J} \frac{1}{J^2}\left[\mathbf{1}\left\{t_1 \le t_2\right\} \Pr\left(\mathrm{Ber}^S_{ij}(t_1) = 1\right) + \mathbf{1}\left\{t_1 > t_2\right\} \Pr\left(\mathrm{Ber}^S_{ij}(t_1) = 1, \tau_i^A(t_2) \neq j\right)\right] \\
&= \frac{1}{J^2}\sum_{t_1=1}^{J}\left[\sum_{t_2=1}^{t_1-1} \Pr\left(\mathrm{Ber}^S_{ij}(t_1) = 1, \mathrm{Ber}^A_{ij}(t_2) = 0\right) + \sum_{t_2=t_1}^{J} \Pr\left(\mathrm{Ber}^S_{ij}(t_1) = 1\right)\right] \\
&= \frac{1}{J^2}\sum_{t_1=1}^{J}\left[\sum_{t_2=1}^{t_1-1} \iota^S_{ij}(1-\iota^A_{ij}) + \sum_{t_2=t_1}^{J} \iota^S_{ij}\right] \\
&= \frac{1}{J^2}\sum_{t_1=1}^{J}\left[(t_1-1)\iota^S_{ij}(1-\iota^A_{ij}) + (J-t_1+1)\iota^S_{ij}\right] \\
&= \frac{1}{J^2}\sum_{t_1=1}^{J}\left[J\iota^S_{ij} - (t_1-1)\iota^S_{ij}\iota^A_{ij}\right] \\
&= \iota^S_{ij} - \iota^S_{ij}\iota^A_{ij}\frac{1}{J^2}\sum_{t_1=1}^{J}(t_1-1) \\
&= \iota^S_{ij} - \iota^S_{ij}\iota^A_{ij}\frac{1}{J^2}\left(\frac{J(J+1)}{2} - J\right) \\
&= \iota^S_{ij}\left(1 - \frac{J-1}{2J}\iota^A_{ij}\right).
\end{aligned}
$$

Note that we use the independence of the two random permutations and the two multinomial distributions. The similar calculation yields the result. □

A.6 Proof of Proposition 4

Lemma 2. *Fix (i,j) and a period with subperiods $t = 1, \ldots, J$. For each rule $k \in \{S, A\}$ let $\tilde{R}^D_{k,i,t} \subseteq J$ be the realized spot–exposure set at t. Under the fastest–first policy with tie to S, define the realized doctor-side set at t by*

$$
\mathbf{1}\{\, j \in \tilde{R}^{D,\mathrm{first}}_{i,t} \,\} = \mathbf{1}\Big\{\, j \in \tilde{R}^D_{S,i,t} \;\wedge\; j \notin \bigcup_{u<t} \tilde{R}^D_{A,i,u} \,\Big\} + \mathbf{1}\Big\{\, j \in \tilde{R}^D_{A,i,t} \;\wedge\; j \notin \bigcup_{u\le t} \tilde{R}^D_{S,i,u} \,\Big\}. \tag{$\star$}
$$

Then

$$
\sum_{t=1}^{J} \mathbb{E}\big[\mathbf{1}\{j \in \tilde{R}^{D,\mathrm{first}}_{i,t}\}\big] = \iota^S_{ij} + \iota^A_{ij} - \iota^S_{ij}\iota^A_{ij}.
$$

Proof. By construction, $\sum_t \mathbf{1}\{j \in \tilde{R}^{D,\mathrm{first}}_{i,t}\} \in \{0,1\}$ and

$$
\sum_{t=1}^{J} \mathbf{1}\{j \in \tilde{R}^{D,\mathrm{first}}_{i,t}\} = \mathbf{1}\Big\{\, j \in \bigcup_t \tilde{R}^D_{S,i,t} \;\text{ or }\; j \in \bigcup_t \tilde{R}^D_{A,i,t} \,\Big\}.
$$

Taking expectations and using independence across rules,

$$\mathbb{E}\Big[\sum_t \mathbf{1}\{j \in \tilde{R}^{D,\text{first}}_{i,t}\}\Big] = \Pr\Big(j \in \bigcup_t \tilde{R}^D_{S,i,t}\Big) + \Pr\Big(j \in \bigcup_t \tilde{R}^D_{A,i,t}\Big) - \Pr\Big(j \in \bigcup_t \tilde{R}^D_{S,i,t}\Big)\Pr\Big(j \in \bigcup_t \tilde{R}^D_{A,i,t}\Big)$$
$$= \iota^S_{ij} + \iota^A_{ij} - \iota^S_{ij}\iota^A_{ij}.$$

□

Proof of Proposition 4. Fix doctor i and consider the one-period Bellman equation with J subperiods:

$$\alpha^D_i = \rho\,\mathbb{E}\Big[\mathbf{1}\{\emptyset = \tilde{R}^{D,\text{first}}_{i,t}\}\,\alpha^D_i + \sum_{j=1}^{J}\Big\{\alpha^D_i + \mathbf{1}\{j \in \tilde{R}^{D,\text{first}}_{i,t}\}\,\mathbf{1}\{V^{\text{det}}_{ji} + \varepsilon^P > \alpha^P_j\}\,\max\{\tilde{U}^{\text{det}}_{ij} - \kappa\alpha^D_i + \varepsilon^D, 0\}\Big\}\Big],$$

where stationarity allows us to omit time subscripts on primitives. Averaging over subperiods, Lemma 2 yields

$$\frac{1}{J}\sum_{t=1}^{J}\mathbb{E}[\mathbf{1}\{j \in \tilde{R}^{D,\text{first}}_{i,t}\}] = \frac{\widehat{\iota}_{ij}}{J}, \qquad \frac{1}{J}\sum_{t=1}^{J}\mathbb{E}[\mathbf{1}\{\emptyset = \tilde{R}^{D,\text{first}}_{i,t}\}] = 1 - \frac{1}{J}\sum_{j=1}^{J}\widehat{\iota}_{ij}.$$

Assuming independent Gumbel shocks $\varepsilon^D, \varepsilon^P$ with scales ζ^D, ζ^P, and writing $\tilde{U}^{\text{det}}_{ij} = X'_{ij}\beta^D + Z'_{ij}\delta^D$ and $V^{\text{det}}_{ji} = X'_{ij}\beta^P + Z'_{ij}\delta^P$, we have

$$P^P_{ji}(\theta;\alpha^P_j) := \Pr(V^{\text{det}}_{ji} + \varepsilon^P > \alpha^P_j), \qquad \mathbb{E}[\max\{\tilde{U}^{\text{det}}_{ij} - \kappa\alpha^D_i + \varepsilon^D, 0\}] = \zeta^D \ln\Big(1 + e^{(\tilde{U}^{\text{det}}_{ij} - \kappa\alpha^D_i)/\zeta^D}\Big).$$

Substituting and moving the "no-exposure" term to the left gives

$$(1-\rho)\alpha^D_i = \rho\sum_{j=1}^{J}\frac{\widehat{\iota}_{ij}}{J}\,P^P_{ji}(\theta;\alpha^P_j)\,\zeta^D \ln\Big(1 + e^{(X'_{ij}\beta^D + Z'_{ij}\delta^D - \kappa\alpha^D_i)/\zeta^D}\Big),$$

which is the first line of (6).

For the post side, the analogous Bellman equation and the large-market collision correction τ imply

$$\frac{1}{J}\sum_{t=1}^{J}\mathbb{E}[\mathbf{1}\{i \in \tilde{R}^{P,\text{first}}_{j,t}\}] = \frac{\tau\,\widehat{\iota}_{ij}}{J}.$$

Using

$$P^D_{ij}(\theta;\alpha^D_i) := \Pr(\tilde{U}^{\text{det}}_{ij} + \varepsilon^D > \kappa\alpha^D_i), \qquad \mathbb{E}[\max\{V^{\text{det}}_{ji} - \alpha^P_j + \varepsilon^P, 0\}] = \zeta^P \ln\Big(1 + e^{(V^{\text{det}}_{ji} - \alpha^P_j)/\zeta^P}\Big),$$

the same rearrangement yields the second line of (6). □

A.7 Contraction Property

Theorem 3. *Consider the stationary system* (6) *with*

$$\widehat{\iota}_{ij} = \iota^S_{ij} + \iota^A_{ij} - \iota^S_{ij}\iota^A_{ij}, \qquad P^D_{ij}(\theta;\alpha^D_i) = \sigma\Big(\frac{X'_{ij}\beta^D + Z'_{ij}\delta^D - \kappa\alpha^D_i}{\zeta^D}\Big), \qquad P^P_{ji}(\theta;\alpha^P_j) = \sigma\Big(\frac{X'_{ij}\beta^P + Z'_{ij}\delta^P - \alpha^P_j}{\zeta^P}\Big),$$

$$\psi^D_{ij}(\alpha^D_i) := \zeta^D \log\Big(1 + e^{\frac{X'_{ij}\beta^D + Z'_{ij}\delta^D - \kappa\alpha^D_i}{\zeta^D}}\Big), \qquad \psi^P_{ij}(\alpha^P_j) := \zeta^P \log\Big(1 + e^{\frac{X'_{ij}\beta^P + Z'_{ij}\delta^P - \alpha^P_j}{\zeta^P}}\Big), \quad \sigma(x) := \frac{1}{1+e^{-x}}.$$

Assume:

(A1) ***Bounded indices.*** *There exist $M_D, M_P > 0$ such that $|X'_{ij}\beta^D + Z'_{ij}\delta^D| \le M_D$ and $|X'_{ij}\beta^P + Z'_{ij}\delta^P| \le M_P$ for all (i,j).*

(A2) ***Scales.*** *$\zeta^D, \zeta^P > 0$, $\kappa \in (0,1]$, $\rho \in (0,1)$.*

(A3) ***Exposure sensitivity.*** *The union exposure $\widehat{\iota}_{ij}(\theta; \alpha_i^D, \alpha_j^P)$ is (globally) Lipschitz in its arguments with*

$$\big|\partial_{\alpha_i^D}\widehat{\iota}_{ij}\big| \;\le\; \frac{L_{\widehat{\iota}}^{(D)}}{J}, \qquad \big|\partial_{\alpha_j^P}\widehat{\iota}_{ij}\big| \;\le\; \frac{L_{\widehat{\iota}}^{(P)}}{J} \qquad \text{for all } (i,j),$$

for some constants $L_{\widehat{\iota}}^{(D)}, L_{\widehat{\iota}}^{(P)} \ge 0$ that do not depend on I, J.

For $R > 0$ define $B_R := \{\alpha : \|\alpha\|_\infty \le R\}$ and

$$B_D(R) := \sup_{|a|\le R} \zeta^D \log\Big(1 + e^{\frac{M_D + \kappa|a|}{\zeta^D}}\Big), \qquad B_P(R) := \sup_{|b|\le R} \zeta^P \log\Big(1 + e^{\frac{M_P + |b|}{\zeta^P}}\Big),$$

and the exposure masses

$$\gamma_{\max}^D := \max_i \frac{1}{J}\sum_j \widehat{\iota}_{ij}, \qquad \gamma_{\max}^P := \max_j \frac{\tau}{J}\sum_i \widehat{\iota}_{ij}.$$

Then the map $g = (g^D, g^P)$ given by the right-hand side of (6) satisfies:

(i) Self–mapping. *If R obeys*

$$R \;\ge\; \max\Big\{\frac{\rho}{1-\rho}\,\gamma_{\max}^D\, B_D(R), \quad \frac{\rho\,\tau}{1-\rho}\,\gamma_{\max}^P\, B_P(R)\Big\}, \tag{$\star$}$$

then $g(B_R) \subseteq B_R$.

(ii) Lipschitz bound. *For all $\alpha, \alpha' \in B_R$,*

$$\|g(\alpha) - g(\alpha')\|_\infty \;\le\; q_R\,\|\alpha - \alpha'\|_\infty,$$

with

$$\begin{aligned} q_R \;:=\; \max\Big\{ &\frac{\rho}{1-\rho}\Big[\,\gamma_{\max}^D L_\psi^D \;+\; B_D(R)\Big(\tfrac{L_{\widehat{\iota}}^{(D)}}{J} + \tfrac{L_{\widehat{\iota}}^{(P)}}{J} + \gamma_{\max}^D L_P^{(P)}\Big)\,\Big], \\ &\frac{\rho\,\tau}{1-\rho}\Big[\,\gamma_{\max}^P L_\psi^P \;+\; B_P(R)\Big(\tfrac{L_{\widehat{\iota}}^{(D)}}{J} + \tfrac{L_{\widehat{\iota}}^{(P)}}{J} + \gamma_{\max}^P L_P^{(D)}\Big)\,\Big]\,\Big\}, \end{aligned}$$

where the component-wise global Lipschitz moduli satisfy

$$L_\psi^D \le \kappa, \qquad L_\psi^P \le 1, \qquad L_P^{(D)} \le \frac{\kappa}{4\zeta^D}, \qquad L_P^{(P)} \le \frac{1}{4\zeta^P}.$$

(iii) Contraction and uniqueness. *If $q_R < 1$, then g is a contraction on B_R and the stationary system (6) admits a unique fixed point $\alpha^\star \in B_R$.*

Proof. (i) Using $\widehat{\iota}_{ij} \in [0,1]$ and $\frac{1}{J}\sum_j \widehat{\iota}_{ij} \le \gamma_{\max}^D$,

$$|g_i^D(\alpha)| \le \frac{\rho}{1-\rho}\frac{1}{J}\sum_j \widehat{\iota}_{ij} \sup_{|a|\le R} \psi_{ij}^D(a) \le \frac{\rho}{1-\rho}\,\gamma_{\max}^D\, B_D(R),$$

and similarly $|g_j^P(\alpha)| \le \frac{\rho\,\tau}{1-\rho}\,\gamma_{\max}^P\,B_P(R)$, which yields $(\star)$.

(ii) Write $g_i^D = \frac{\rho}{1-\rho}\sum_j \frac{1}{J} F_{ij}^D(a_i, b_j)$ with

$$F_{ij}^D(a,b) := \widehat{\iota}_{ij}(a,b)\,P_{ji}^P(b)\,\psi_{ij}^D(a), \quad a := \alpha_i^D,\ b := \alpha_j^P.$$

By the product rule and the bounds in the statement,

$$\big|\partial_a F_{ij}^D\big| \le \underbrace{\big|\partial_a \widehat{\iota}_{ij}\big|}_{\le L_{\widehat{\iota}}^{(D)}/J}\,|P_{ji}^P\,\psi_{ij}^D| + \underbrace{|\widehat{\iota}_{ij}|}_{\le 1}\,|P_{ji}^P|\,\underbrace{\big|\partial_a \psi_{ij}^D\big|}_{\le L_\psi^D} \;\le\; \frac{L_{\widehat{\iota}}^{(D)}}{J}\,B_D(R) + L_\psi^D,$$

$$\big|\partial_b F_{ij}^D\big| \le \underbrace{\big|\partial_b \widehat{\iota}_{ij}\big|}_{\le L_{\widehat{\iota}}^{(P)}/J}\,|P_{ji}^P\,\psi_{ij}^D| + \underbrace{|\widehat{\iota}_{ij}|}_{\le 1}\,\underbrace{\big|\partial_b P_{ji}^P\big|}_{\le L_P^{(P)}}\,|\psi_{ij}^D| \;\le\; \frac{L_{\widehat{\iota}}^{(P)}}{J}\,B_D(R) + L_P^{(P)}\,B_D(R).$$

Summing over j and using $\frac{1}{J}\sum_j \widehat{\iota}_{ij} \le \gamma_{\max}^D$ gives

$$\big|g_i^D(\alpha) - g_i^D(\alpha')\big| \le \frac{\rho}{1-\rho}\left[\gamma_{\max}^D\,L_\psi^D + B_D(R)\Big(\tfrac{L_{\widehat{\iota}}^{(D)}}{J} + \tfrac{L_{\widehat{\iota}}^{(P)}}{J} + \gamma_{\max}^D L_P^{(P)}\Big)\right]\|\alpha - \alpha'\|_\infty.$$

The post side follows symmetrically with

$$F_{ij}^P(a,b) := \widehat{\iota}_{ij}(a,b)\,P_{ij}^D(a)\,\psi_{ij}^P(b),$$

and the column mass bound $\frac{\tau}{J}\sum_i \widehat{\iota}_{ij} \le \gamma_{\max}^P$, plus $|\partial_a P_{ij}^D| \le L_P^{(D)}$. Taking the max of the two sides yields the stated q_R. (iii) is an application of Banach's fixed-point theorem. □

Corollary (logistic S/A rules). If each rule is logistic in its "own" side,

$$\iota_{ij}^S = \frac{1}{J}\,\sigma\Big(\frac{X_{ij}'\beta^D + Z_{ij}'\delta^S - \kappa\alpha_i^D}{\zeta^S}\Big), \qquad \iota_{ij}^A = \frac{1}{J}\,\sigma\Big(\frac{X_{ij}'\beta^P + Z_{ij}'\delta^A - \alpha_j^P}{\zeta^A}\Big),$$

then, using $\sigma'(x) \le 1/4$ and the product formula for $\widehat{\iota}$,

$$L_{\widehat{\iota}}^{(D)} \;\le\; \frac{\kappa}{4\zeta^S}, \qquad L_{\widehat{\iota}}^{(P)} \;\le\; \frac{1}{4\zeta^A},$$

so Assumption (A3) holds with the same $1/J$ scaling as in the multinomial case.

B Sinkhorn Algorithm

Sinkhorn scaling takes a strictly positive matrix $K \in \mathbb{R}_{++}^{I\times J}$ and target marginals $r \in \mathbb{R}_{++}^I$, $c \in \mathbb{R}_{++}^J$ with $\sum_i r_i = \sum_j c_j$, and finds diagonal scalings $u > 0$, $v > 0$ such that

$$\mu \;=\; \mathrm{diag}(u)\,K\,\mathrm{diag}(v) \quad \text{satisfies} \quad \mu\mathbf{1} = c, \qquad \mathbf{1}^\top\mu = r^\top.$$

Equivalently, it computes the *KL projection* of K onto the set of matrices with row/column sums (r, c):

$$\mu \;=\; \arg\min_{\tilde{\mu}\geq 0} \sum_{i,j} \tilde{\mu}_{ij} \ln \frac{\tilde{\mu}_{ij}}{K_{ij}} \quad \text{s.t.} \quad \tilde{\mu}\mathbf{1} = c,\ \mathbf{1}^\top \tilde{\mu} = r^\top.$$

Algorithm (alternating row/column scaling). Given $K > 0$, $r > 0$, $c > 0$ with $\sum r = \sum c$, initialize $v \leftarrow \mathbf{1}_J$. Repeat until convergence:

$$u \leftarrow r \oslash (Kv), \qquad v \leftarrow c \oslash (K^\top u),$$

where $\oslash$ denotes elementwise division and matrix–vector products are standard. Output $\mu = \mathrm{diag}(u)\, K\, \mathrm{diag}(v)$. When $K > 0$, this iteration converges to the unique scaling (up to a common scalar fixed by the marginals). For numerical stability with extreme values, a log-domain implementation is recommended:

$$\log u_i \leftarrow \log r_i - \mathrm{LSE}_j\big(\log K_{ij} + \log v_j\big), \qquad \log v_j \leftarrow \log c_j - \mathrm{LSE}_i\big(\log K_{ij} + \log u_i\big),$$

where $\mathrm{LSE}(z) = \log \sum_k e^{z_k}$.

Tiny worked example (2×2) Target row/column sums are $r = c = (1, 1)$. Take

$$K = \begin{pmatrix} 1 & 2 \\ 3 & 4 \end{pmatrix}.$$

Let's look a t the first iteration. Start with $v = (1, 1)$.

$$Kv = \begin{pmatrix} 3 \\ 7 \end{pmatrix}, \qquad u = r \oslash (Kv) = \Big(\tfrac{1}{3},\ \tfrac{1}{7}\Big).$$

$$K^\top u = \begin{pmatrix} 1 & 3 \\ 2 & 4 \end{pmatrix} \begin{pmatrix} \frac{1}{3} \\ \frac{1}{7} \end{pmatrix} = \begin{pmatrix} \frac{16}{21} \\ \frac{26}{21} \end{pmatrix}, \qquad v = c \oslash (K^\top u) = \Big(\tfrac{21}{16},\ \tfrac{21}{26}\Big) \approx (1.3125,\ 0.8077).$$

Scaled matrix:

$$\mu = \mathrm{diag}(u)\, K\, \mathrm{diag}(v) \approx \begin{pmatrix} 0.4375 & 0.5385 \\ 0.5625 & 0.4615 \end{pmatrix},$$

with row sums $\approx (0.976,\ 1.024)$ and column sums exactly $(1, 1)$.

Repeating the two updates quickly brings both rows and columns to $(1, 1)$. In this example, after a couple of iterations, $\mu \approx \left[\begin{smallmatrix} 0.4494 & 0.5506 \\ 0.5506 & 0.4494 \end{smallmatrix}\right]$.

C Detail of Estimation

Let $\ell_n(\theta)$ be the (negative) average log-likelihood (so we minimize ℓ_n), and let $\hat{\theta}$ be a local minimizer. The observed information (for MLE under correct specification) is $H_n(\hat{\theta}) := \nabla^2 \ell_n(\hat{\theta})$; the usual covariance estimator is $\widehat{\mathrm{Var}}(\hat{\theta}) \approx H_n(\hat{\theta})^{-1}$. In practice $p := \dim(\theta)$ can be large and we only need variances or covariances for a few components or a smooth scalar functional $g(\theta)$. This section shows how to compute *selected columns* of H^{-1} without forming H, using Hessian–vector products (HVPs) and a linear solver

(conjugate gradient, CG).

Lemma 3. *Let $H \in \mathbb{R}^{p\times p}$ be invertible and e_i the i-th canonical basis vector. The unique solution x to the linear system $Hx = e_i$ equals the i-th column of H^{-1}.*

Proof. By definition $H^{-1}e_i$ is the i-th column of H^{-1} and satisfies $H(H^{-1}e_i) = e_i$. By uniqueness of solutions for invertible H, $x = H^{-1}e_i$. □

Corollary. For any index set $S \subset \{1, \dots, p\}$, solving $Hx = e_s$ for all $s \in S$ returns the submatrix $H^{-1}_{S,S}$ via column extraction.

Thus, to obtain a 2×2 covariance block for (θ_i, θ_j), one solves $Hx = e_i$ and $Hx = e_j$ and reads off

$$\begin{pmatrix} (H^{-1})_{ii} & (H^{-1})_{ij} \\ (H^{-1})_{ji} & (H^{-1})_{jj} \end{pmatrix}.$$

C.1 Hessian–vector products and CG

Forming H explicitly is $O(p^2)$ memory and $O(p^2)$ time. Instead, we use an *oracle* for HVPs

$$v \;\mapsto\; Hv \;=\; \nabla^2 \ell_n(\hat{\theta})\, v,$$

and apply a Krylov solver (e.g. conjugate gradient) to each right-hand side e_s. Modern autodiff frameworks provide HVPs at the cost of a few reverse/forward passes (Pearlmutter's trick):

$$Hv \;=\; \mathrm{d}\big[\nabla \ell_n(\theta)\big]_{\theta=\hat{\theta}}[v].$$

When H is positive definite, CG converges rapidly; for numerical stability one can solve

$$(H + \lambda I)x = e_s \quad (\lambda > 0),$$

which returns $(H + \lambda I)^{-1}$-columns, a Tikhonov-regularized approximation to H^{-1}. Small λ yields negligible bias and improved conditioning. Preconditioning further accelerates convergence but is optional.

C.2 Delta method with selected blocks

Let $g : \mathbb{R}^p \to \mathbb{R}$ be differentiable, and suppose g depends only on a small subset S of parameters. By the delta method,

$$\mathrm{Var}\big(g(\hat{\theta})\big) \;\approx\; \nabla g(\hat{\theta})^\top\, H(\hat{\theta})^{-1}\, \nabla g(\hat{\theta}).$$

If $\nabla g(\hat{\theta})$ has support in S, then only $H^{-1}_{S,S}$ is needed:

$$\mathrm{Var}\big(g(\hat{\theta})\big) \;\approx\; \big(\nabla_S g(\hat{\theta})\big)^\top\, H^{-1}_{S,S}\, \nabla_S g(\hat{\theta}).$$

Hence it suffices to solve $Hx = e_s$ for $s \in S$, stack the resulting columns into $C = [H^{-1}e_s]_{s\in S}$, and compute $\mathrm{Var}(g) \approx (\nabla_S g)^\top C\, \nabla_S g$. This yields standard errors and z-scores for $g(\hat{\theta})$ without ever materializing the full H or its inverse.

C.3 Extensions: sandwich and quasi-ML

Under correct specification, the MLE satisfies $S(\hat{\theta}) = H(\hat{\theta})$, where

$$S(\hat{\theta}) \;=\; \frac{1}{n}\sum_{t=1}^{n} s_t(\hat{\theta}) s_t(\hat{\theta})^\top, \quad H(\hat{\theta}) \;=\; \nabla^2 \ell_n(\hat{\theta}),$$

so $\mathrm{Var}(\hat{\theta}) \approx H^{-1}$. For misspecification or dependent data, the robust (sandwich) variance is

$$\mathrm{Var}(\hat{\theta}) \;\approx\; H^{-1} S\, H^{-1}.$$

The same column-solve idea applies: one can obtain $H^{-1}u$ for any vector u by solving $Hx = u$ with CG+HVP. Thus, products like $H^{-1}SH^{-1}$ with a vector can be built without forming any large dense matrices.[7]

C.4 Profile likelihood / NFXP remark

In nested fixed-point (NFXP) settings, a nuisance object $\alpha(\theta)$ is defined implicitly by a contraction mapping. If the outer objective uses the *profile* criterion $\ell_n(\theta, \alpha(\theta))$, then the observed profile Hessian w.r.t. θ plays the role of $H(\hat{\theta})$ above. In practice one often treats a numerically converged $\hat{\alpha}$ as fixed ("K-step" M-estimation), and computes H as the θ-Hessian of $\ell_n(\theta; \hat{\alpha})$. Under standard regularity (contraction, inner-loop convergence, and smoothness), this differs from the exact profile Hessian by $o_p(1)$, so the same HVP+CG method consistently recovers the needed inverse blocks.

C.5 Algorithmic summary

1. Compute $\hat{\theta}$ and fix the nuisance $\hat{\alpha}$ if applicable (profile or K-step).
2. Implement an HVP oracle $v \mapsto Hv$ for $H = \nabla^2_{\theta\theta} \ell_n(\hat{\theta}; \hat{\alpha})$.
3. For indices S of interest, solve $(H + \lambda I)x = e_s$ by CG, using only HVPs. Stack the solutions as columns to obtain an approximation to $H^{-1}_{\cdot S}$.
4. Read off $H^{-1}_{S,S}$; apply the delta method to any $g(\theta)$ whose gradient is supported on S.

D Solve Adjoint Equation

In each outer iteration of the optimization, the adjoint vector π solves

$$M^\top \pi = \mathbf{1}, \qquad M = \begin{bmatrix} A & B \\ C & D \end{bmatrix} \in \mathbb{R}^{(I+J)\times(I+J)}.$$

In our model, thanks to the fixed-point Jacobian structure:

- $A \in \mathbb{R}^{I\times I}$ and $D \in \mathbb{R}^{J\times J}$ are **diagonal** (with positive entries),

[7] For example, to extract a 2×2 block of $H^{-1}SH^{-1}$, compute $c_i = H^{-1}e_i$ and $c_j = H^{-1}e_j$, then assemble $[c_i, c_j]^\top S[c_i, c_j]$.

- $B \in \mathbb{R}^{I\times J}$ and $C \in \mathbb{R}^{J\times I}$ are dense but their products can be formed in $O(IJ)$.

This is ideal for avoiding an $O((I+J)^3)$ dense solve of $M^\top$ by using **Schur complements** to reduce the system to dimension $\min\{I, J\}$.

D.1 Solving on the P-side (size J)

Write $\pi = \begin{bmatrix} \pi_D \\ \pi_P \end{bmatrix}$ and

$$\begin{bmatrix} A^\top & C^\top \\ B^\top & D^\top \end{bmatrix} \begin{bmatrix} \pi_D \\ \pi_P \end{bmatrix} = \begin{bmatrix} \mathbf{1}_I \\ \mathbf{1}_J \end{bmatrix}.$$

From the first block: $\pi_D = (A^\top)^{-1}(\mathbf{1}_I - C^\top \pi_P)$. Substituting into the second block gives

$$\underbrace{\big(D^\top - B^\top (A^\top)^{-1} C^\top\big)}_{S_P^\top} \pi_P \;=\; \mathbf{1}_J - B^\top (A^\top)^{-1} \mathbf{1}_I.$$

Hence

$$\pi_P = (S_P^\top)^{-1}\Big(\mathbf{1}_J - B^\top (A^\top)^{-1}\mathbf{1}_I\Big), \qquad \pi_D = (A^\top)^{-1}\big(\mathbf{1}_I - C^\top \pi_P\big).$$

Here A is diagonal, so $(A^\top)^{-1} = \mathrm{diag}(1/\mathrm{diag}(A))$ is trivial. $S_P = D - B^\top A^{-1} C^\top$ is $J \times J$, so if $J \le I$ this is much cheaper than a full $(I+J)$-system.

D.2 Solving on the D-side (size I)

Similarly, from the second block: $\pi_P = (D^\top)^{-1}(\mathbf{1}_J - B^\top \pi_D)$. Substitute into the first block:

$$\underbrace{\big(A^\top - C^\top (D^\top)^{-1} B^\top\big)}_{S_D^\top} \pi_D \;=\; \mathbf{1}_I - C^\top (D^\top)^{-1} \mathbf{1}_J,$$

$$\pi_D = (S_D^\top)^{-1}\Big(\mathbf{1}_I - C^\top (D^\top)^{-1}\mathbf{1}_J\Big), \qquad \pi_P = (D^\top)^{-1}\big(\mathbf{1}_J - B^\top \pi_D\big).$$

Again D is diagonal $\Rightarrow (D^\top)^{-1}$ is trivial; this is preferable if $I \le J$.

Complexity and Memory

- Dense direct solve: $\mathcal{O}((I + J)^3)$ time, $\mathcal{O}((I + J)^2)$ memory.
- Schur complement: building costs about $\mathcal{O}(IJ \min\{I, J\})$; solve costs $\mathcal{O}(\min\{I, J\}^3)$.
- Diagonal blocks A, D make inverses $\mathcal{O}(I + J)$.

Because $I \neq J$ in practice, picking the smaller side gives a substantial speedup.

D.3 Iterative Solvers: GMRES

$M^\top$ is generally non-symmetric and not SPD, so the conjugate gradient method is unsuitable, but GMRES works well. Use a *block-Jacobi* preconditioner $P \approx \mathrm{diag}(A, D)$ and implement only mat-

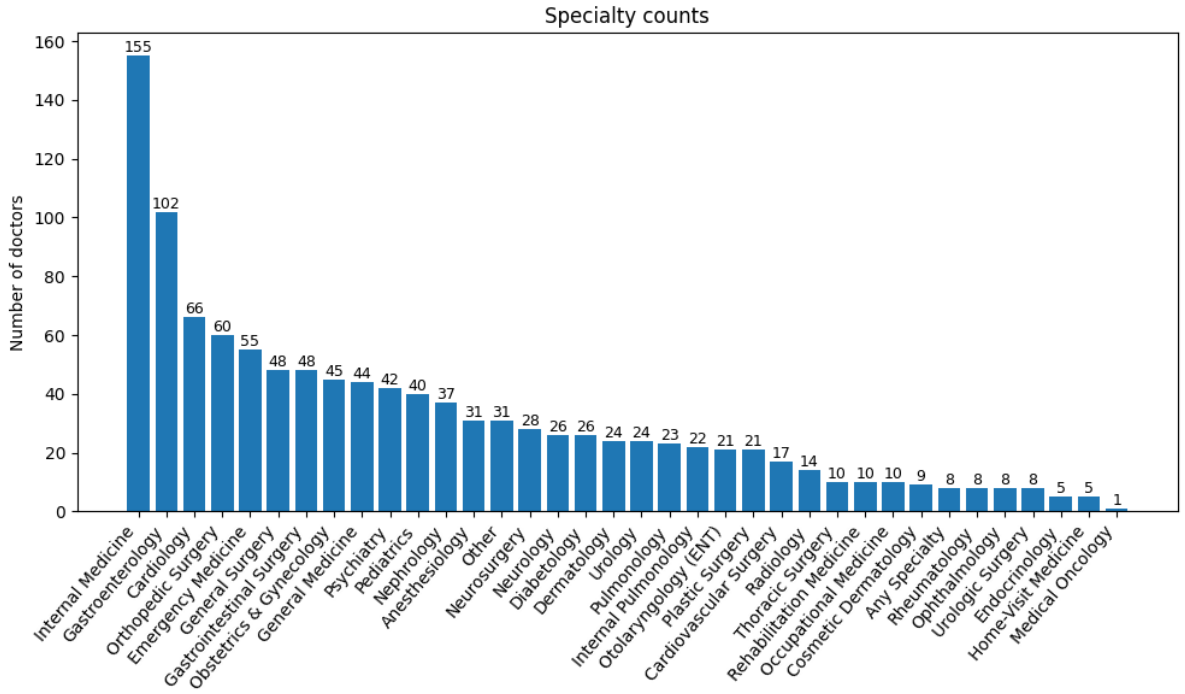

Figure E.1

rix–vector products in $O(IJ)$:

$$\text{matvec: } x = \begin{bmatrix} x_D \\ x_P \end{bmatrix} \mapsto \begin{bmatrix} Ax_D + C^\top x_P \\ B^\top x_D + Dx_P \end{bmatrix}, \qquad \text{prec: } r \mapsto \begin{bmatrix} A^{-1} r_D \\ D^{-1} r_P \end{bmatrix}.$$

Pseudo-code Snippet For the P-side ($J \times J$) solve:

Input: $A = \mathrm{diag}(a),\ D = \mathrm{diag}(d),\ B \in \mathbb{R}^{I \times J},\ C \in \mathbb{R}^{J \times I}$.

Step 1: $\mathrm{BA} \leftarrow A^{-1}$ scales columns of B $\quad (\mathrm{BA} = A^{-1}B)$.

Step 2: $T \leftarrow \mathrm{BA}^\top C^\top \in \mathbb{R}^{J \times J}$.

Step 3: $S_P \leftarrow D - T$.

Step 4: $r \leftarrow \mathbf{1}_J - B^\top A^{-1} \mathbf{1}_I$.

Step 5: $\pi_P \leftarrow (S_P^\top)^{-1} r$ $(\Leftrightarrow S_P^\top \pi_P = r)$.

Step 6: $\pi_D \leftarrow A^{-1}(\mathbf{1}_I - C^\top \pi_P)$.

E Additional Figures

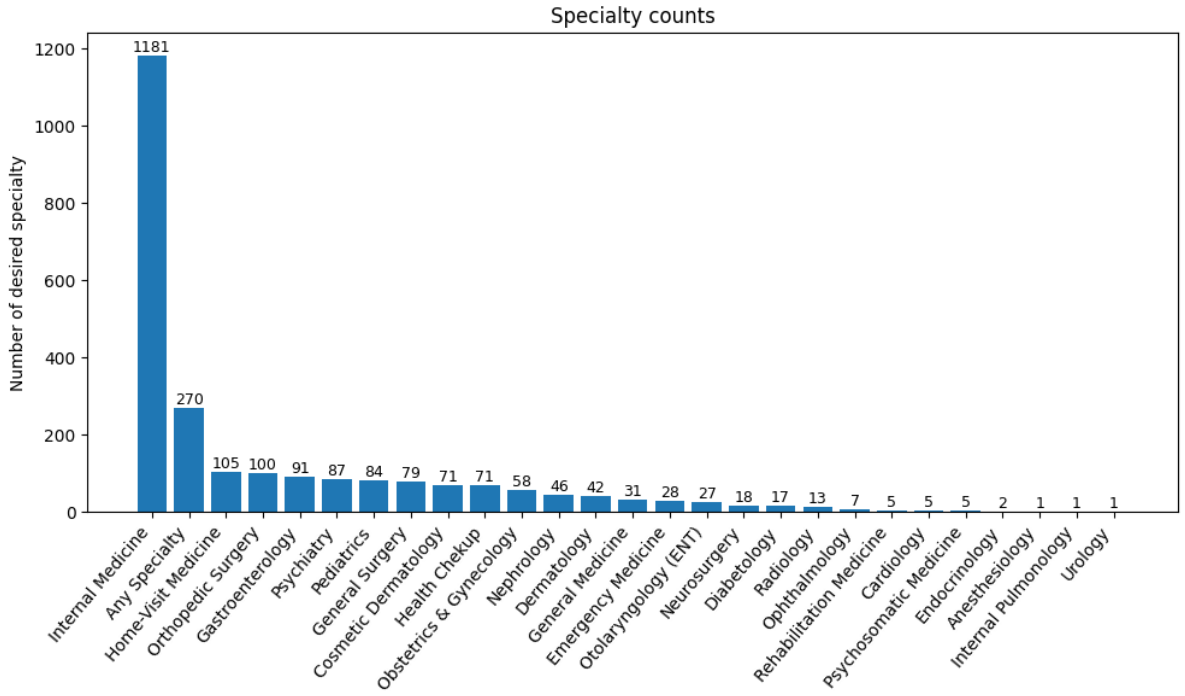

Figure E.2

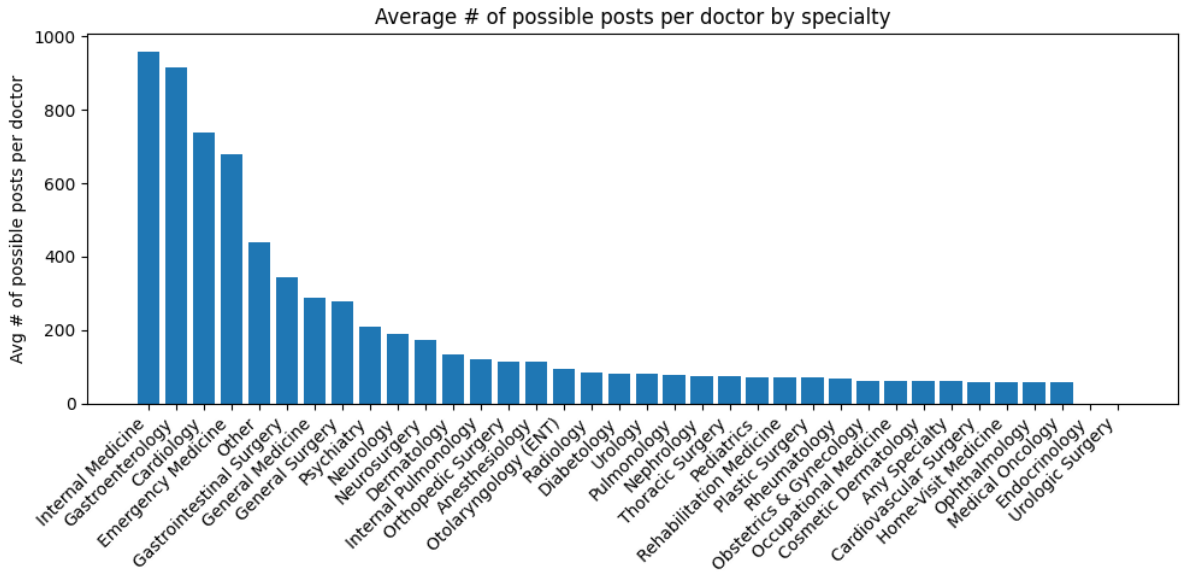

Figure E.3

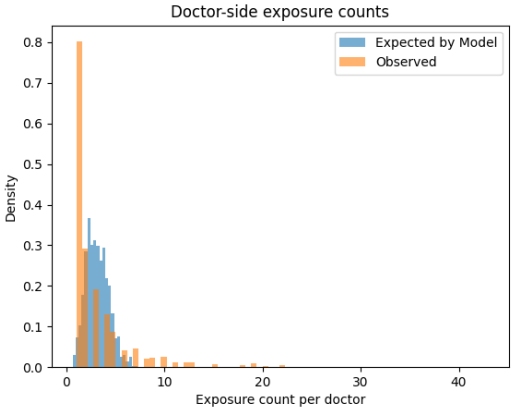

Panel A: Doctor counts

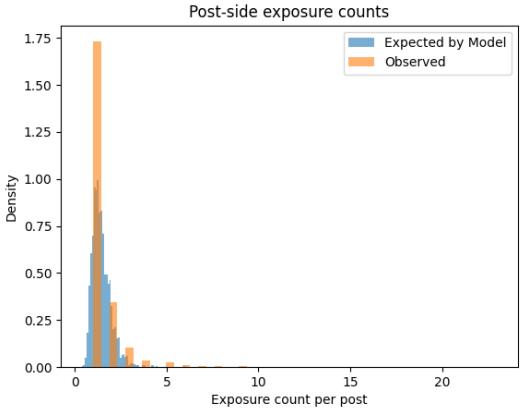

Panel B: Post counts

Figure E.4. Observed vs. expected exposure counts by side

Table E.1. Equivalence change in other covariates to a 10% increase in salary

Side	Variable	Equiv. (raw)	SE	z	p
Panel A: Self-search Exposure (Doctor)					
Doctor	Outpatient care	0.0715	0.0181	3.9584	0.0001
Doctor	Home-visit medical care	0.0403	0.0130	3.1041	0.0019
Doctor	Inpatient ward care	0.0309	0.0065	4.7756	0.0000
Doctor	Dialysis	0.0094	0.0020	4.6866	0.0000
Doctor	Health checkup	0.0417	0.0103	4.0601	0.0000
Doctor	Endoscopic surgery	0.0122	0.0027	4.4275	0.0000
Doctor	Surgery	−0.0298	0.0248	−1.2020	0.2294
Doctor	House calls	0.1540	0.2549	0.6042	0.5457
Doctor	Image interpretation (radiology)	0.0115	0.0028	4.1060	0.0000
Doctor	Self-pay care	0.0148	0.0033	4.5386	0.0000
Panel B: Agency-recommendation Exposure (Post)					
Post	Outpatient care	−0.1454	0.0559	−2.6007	0.0093
Post	Home-visit medical care	0.1075	0.0806	1.3328	0.1826
Post	Inpatient ward care	−0.0512	0.0118	−4.3296	0.0000
Post	Dialysis	−0.0127	0.0026	−4.8369	0.0000
Post	Health checkup	−0.1145	0.0587	−1.9497	0.0512
Post	Endoscopic surgery	−0.0152	0.0032	−4.7186	0.0000
Post	Surgery	0.1996	0.3953	0.5048	0.6137
Post	House calls	−0.0480	0.0194	−2.4738	0.0134
Post	Image interpretation (radiology)	−0.1210	0.1422	−0.8504	0.3951
Post	Self-pay care	−0.0163	0.0032	−5.0418	0.0000
Panel C: Acceptance (Doctor)					
Doctor	Outpatient care	−0.0133	0.1447	−0.0919	0.9268
Doctor	Home-visit medical care	0.0015	0.0167	0.0921	0.9266
Doctor	Inpatient ward care	−0.0026	0.0278	−0.0922	0.9265
Doctor	Dialysis	−0.0030	0.0324	−0.0922	0.9266
Doctor	Health checkup	0.0017	0.0182	0.0922	0.9266
Doctor	Endoscopic surgery	−0.0017	0.0183	−0.0922	0.9266
Doctor	Surgery	−0.0123	0.1344	−0.0912	0.9274
Doctor	House calls	−0.0030	0.0327	−0.0921	0.9266
Doctor	Image interpretation (radiology)	0.0021	0.0231	0.0922	0.9266
Doctor	Self-pay care	−0.0261	0.2898	−0.0899	0.9284
Panel D: Acceptance (Post)					
Post	Outpatient care	0.5007	0.3015	1.6608	0.0968
Post	Home-visit medical care	0.0491	0.0079	6.2349	0.0000
Post	Inpatient ward care	17.2355	368.8461	0.0467	0.9627
Post	Dialysis	−7.7758	96.3487	−0.0807	0.9357
Post	Health checkup	0.0885	0.0164	5.3911	0.0000
Post	Endoscopic surgery	−0.1385	0.0363	−3.8215	0.0001
Post	Surgery	2.2045	8.7175	0.2529	0.8004
Post	House calls	0.1336	0.0347	3.8524	0.0001
Post	Image interpretation (radiology)	0.2567	0.1213	2.1166	0.0343
Post	Self-pay care	0.0262	0.0038	6.8816	0.0000

Notes: Entries report, for each covariate, the change in raw units that yields the same change in the matching utility term as a 10% increase in salary. Standard errors use the fixed-α outer likelihood with observed information, and are mapped to the reported statistics via the delta method.

Table E.2. Determinants of salary offsets

	Post	**Doctor**
On call	0.0422^{***}	—
	(0.0061)	
Hours	-0.0036^{***}	—
	(0.0002)	
Age	—	-0.0109^{*}
		(0.0053)
Experience	—	0.0424^{***}
		(0.0054)
Service/feature indicators		
Outpatient care	-0.0235^{***}	0.3849^{***}
	(0.0035)	(0.0482)
Inpatient ward care	-0.0207^{***}	0.4677^{***}
	(0.0053)	(0.0506)
Health checkup	-0.0357^{***}	0.2200^{***}
	(0.0051)	(0.0445)
Radiology reading	0.0154	0.1221
	(0.0140)	(0.0811)
Home-visit medical care	-0.0609^{***}	0.0293
	(0.0071)	(0.0563)
House calls	0.0207^{*}	0.0105
	(0.0096)	(0.0669)
Endoscopic surgery	-0.0208^{**}	0.4667^{***}
	(0.0080)	(0.0756)
Dialysis	-0.0532^{***}	0.2306^{***}
	(0.0102)	(0.0588)
Surgery	−0.0369	−0.0734
	(0.0389)	(0.0869)
Self-pay care	-0.0540^{***}	0.2606^{***}
	(0.0074)	(0.0552)
Industrial physician	0.0000	−0.0765
	(0.0000)	(0.0661)

Notes: Entries are OLS coefficients for salary offsets on post-/doctor-side attributes; standard errors in parentheses. Stars: $^{***}p < 0.001$, $^{**}p < 0.01$, $^{*}p < 0.05$. "—" indicates the covariate is not included on that side.

Algorithm 1 Nested Fixed-Point Bregman–Dykstra Annealing

Require: baseline $q \in (0,\infty)^{I\times J}$, initial $\mu^{(0)} \in \mathcal{B}$, bounds $(l^r, c^r) \in \mathbb{R}_+^I$, $(l^c, c^c) \in \mathbb{R}_+^J$, initial temperature $\varepsilon_0 > 0$, cooling $\gamma \in (0,1)$, tolerances $\tau_{\mathrm{FP}}, \tau_{\mathrm{KKT}}$, damping $\theta \in (0,1]$

$t \leftarrow 0$, $\varepsilon \leftarrow \varepsilon_0$

repeat

Value step: solve $G(\alpha^{(t)}, \mu^{(t)}) = 0$ for $\alpha^{(t)}$ (warm start).

Adjoint: form $M^{(t)} = \partial_\alpha G(\alpha^{(t)}, \mu^{(t)})$ and solve

$$M^{(t)\top}\pi^{(t)} = (\mathbf{1}_I, \mathbf{1}_J)^\top.$$

Gradient: compute $\nabla U^{(t)}$:

$$\nabla U_{ij}^{(t)} = \frac{\rho}{J}\Big[\, \pi_i^{D,(t)}\big(W_{ij}^D - \alpha_i^{D,(t)}\big) + \Big(\tfrac{J-1}{J}\Big)^{I-1}\pi_j^{P,(t)}\big(W_{ij}^P - \alpha_j^{P,(t)}\big) \,\Big].$$

Kernel: $K^{(t)} \leftarrow q \odot \exp\big(\nabla U^{(t)}/\varepsilon\big)$

BD init: $X \leftarrow K^{(t)}$; initialize KL–Dykstra *shadow variables* $Z^{\mathrm{box}} \leftarrow \mathbf{1}$, $Z^{r,\le} \leftarrow \mathbf{1}$, $Z^{r,\ge} \leftarrow \mathbf{1}$, $Z^{c,\le} \leftarrow \mathbf{1}$, $Z^{c,\ge} \leftarrow \mathbf{1}$ (all $I \times J$).

repeat ▷ Bregman–Dykstra loop (KL projections over constraint sets)

(Box) $Y \leftarrow X \odot Z^{\mathrm{box}}$; $P \leftarrow \mathrm{clip}(Y,\ 0,\ 1)$ elementwise; $Z^{\mathrm{box}} \leftarrow Z^{\mathrm{box}} \odot (Y \oslash P)$; $X \leftarrow P$.

(Row cap) $Y \leftarrow X \odot Z^{r,\le}$; for each i: let $s_i = \sum_j Y_{ij}$ and $\beta_i = \min\{1,\, c_i^r/s_i\}$, set $P_{ij} = \beta_i Y_{ij}$; $Z^{r,\le} \leftarrow Z^{r,\le} \odot (Y \oslash P)$; $X \leftarrow P$.

(Row floor) $Y \leftarrow X \odot Z^{r,\ge}$; for each i: $s_i = \sum_j Y_{ij}$, $\beta_i = \max\{1,\, l_i^r/s_i\}$, $P_{ij} = \beta_i Y_{ij}$; $Z^{r,\ge} \leftarrow Z^{r,\ge} \odot (Y \oslash P)$; $X \leftarrow P$.

(Col cap) $Y \leftarrow X \odot Z^{c,\le}$; for each j: $t_j = \sum_i Y_{ij}$, $\gamma_j = \min\{1,\, c_j^c/t_j\}$, $P_{ij} = \gamma_j Y_{ij}$; $Z^{c,\le} \leftarrow Z^{c,\le} \odot (Y \oslash P)$; $X \leftarrow P$.

(Col floor) $Y \leftarrow X \odot Z^{c,\ge}$; for each j: $t_j = \sum_i Y_{ij}$, $\gamma_j = \max\{1,\, l_j^c/t_j\}$, $P_{ij} = \gamma_j Y_{ij}$; $Z^{c,\ge} \leftarrow Z^{c,\ge} \odot (Y \oslash P)$; $X \leftarrow P$.

(Stopping) $\mathrm{bd\_res} \leftarrow \|X - \hat{X}\|_1$ with $\hat{X}$ previous-X; break if $\mathrm{bd\_res} \le \tau_{\mathrm{FP}}$.

until converged

Set update: $\widehat{\mu}^{(t+1)} \leftarrow X$

Damping: $\mu^{(t+1)} \leftarrow (1-\theta)\,\mu^{(t)} + \theta\,\widehat{\mu}^{(t+1)}$

Residuals: $\mathrm{res}_{\mathrm{FP}} := \|\mu^{(t+1)} - \mathcal{D}_{\mathrm{BD}}(K^{(t)})\|_1$; *stationarity (KKT) surrogate*:

$$\mathrm{res}_{\mathrm{KKT}} := \max_{i,j}\Big|\, \nabla U_{ij}^{(t)} - \varepsilon \ln(\mu_{ij}^{(t+1)}/q_{ij}) - \lambda_i - \eta_j - \xi_{ij} \,\Big|,$$

where dual surrogates are read from the shadows:

$$\lambda_i := -\varepsilon \ln\Big(\bar{Z}_i^{r,\le}\,\bar{Z}_i^{r,\ge}\Big), \quad \eta_j := -\varepsilon \ln\Big(\bar{Z}_j^{c,\le}\,\bar{Z}_j^{c,\ge}\Big), \quad \xi_{ij} := -\varepsilon \ln Z_{ij}^{\mathrm{box}},$$

with $\bar{Z}_i^{r,\bullet}$ (resp. $\bar{Z}_j^{c,\bullet}$) the row (resp. column) geometric means of the corresponding Z (or any consistent aggregation).

if $\mathrm{res}_{\mathrm{FP}} \le \tau_{\mathrm{FP}}$ **and** $\mathrm{res}_{\mathrm{KKT}} \le \tau_{\mathrm{KKT}}$ **then**

$\varepsilon \leftarrow \gamma\,\varepsilon$ ▷ anneal toward 0

end if

$t \leftarrow t + 1$

until $\varepsilon < \varepsilon_{\min}$ **or** (final residuals below tolerance)

return $\mu^\star = \mu^{(t)}$ (at final ε)